

UNLIMITED

AD 640807

TR 66057

FEBRUARY

1966

ROYAL AIRCRAFT ESTABLISHMENT

TECHNICAL REPORT No. 66057

A COMPUTER STUDY OF AUTOMATIC CONTROL ON THE I.L.S. GLIDE PATH

by

G. Musker

Marian Henman

CLEARINGHOUSE
FOR FEDERAL SCIENTIFIC AND
TECHNICAL INFORMATION

Hardcopy	Microfiche		
\$3.00	\$1.50	51	7/8
pp			
ARCHIVE COPY			

DDC
901 27 1966
RECEIVED

MINISTRY OF AVIATION
FARNBOROUGH HANTS

U.D.C. No. 629.13.014.1 : 629.13.087 : 621.396.933.23 : 518.5

ROYAL AIRCRAFT ESTABLISHMENT

Technical Report No. 66057

February 1966

A COMPUTER STUDY OF AUTOMATIC CONTROL ON THE I.L.S. GLIDE PATH

by

G. Musker

Marian Henman

SUMMARY

A computer study is described of the effect on I.L.S. glide path performance of the addition of various damping terms to the glide path control law of a typical autopilot. The control laws used are analysed by a number of techniques and the results achieved by the different techniques are compared. It is shown that the performance can be improved by the addition of either a vertical velocity term coupled with an acceleration term, or a vertical velocity term coupled with a pitch rate term in the control law.

Departmental Reference: HL.70

	<u>CONTENTS</u>	<u>Page</u>
1	INTRODUCTION	3
2	ANALYSIS PROCEDURE	4
	2.1 Choice of gearing values	5
	2.2 Frequency responses	6
	2.3 Statistical results	7
	2.4 Time history	8
3	MODIFICATIONS TO THE CONTROL LAWS	8
4	DETAILED DISCUSSION OF THE RESULTS	9
	4.1 Frequency responses	9
	4.1.1 Response of the aircraft to beam signal	9
	4.1.2 Response to horizontal wind	9
	4.1.3 Response to vertical wind	10
	4.2 Statistical treatment of response to random horizontal wind	11
	4.3 Time history	12
	4.3.1 Approaches in zero wind	12
	4.3.2 Approaches in the presence of a tailwind shear	12
	4.3.3 Approaches in the presence of a headwind shear and a gust	12
	4.4 Effect of an error on the datum rate-of-descent in the control laws using DH	13
5	CONCLUSIONS	14
	Appendix	15
	Symbols	18
	References	19
	Illustrations	Figures 1-30
	Detachable abstract cards	-

1 INTRODUCTION

One of the more important performance parameters of an automatic landing system is the longitudinal position of the touchdown point of the aircraft along the runway. The mean position and the scatter of the touchdown point should be such that the chance is extremely remote of the aircraft either landing short of the runway threshold, i.e. undershooting, or "floating" down the runway so that it over-runs the far end. Whilst the quality of the flare-out manoeuvre can affect the position of the touchdown point, the accuracy of performance achieved on the I.L.S. glide path immediately prior to the flare has a far greater effect. The positional error of the aircraft from the I.L.S. glide path and the rate of change of this error, which is a measure of the error in the aircraft's rate of descent from that required to fly down the glide path, each have a considerable effect on the point of touchdown^{1,2}.

An assessment of the recorded results obtained from full-scale flight trials has shown that the longitudinal scatter of the touchdown point of current automatic landing systems can only be constrained within the limit imposed by Civil safety standards by restricting the wind conditions in which the systems are used. For operational use, wider wind limits are desirable and so an analogue computer study has been made to investigate whether improvements can be made to the accuracy of performance on the I.L.S. glide path. This Report describes the results of the investigation.

One way of improving beam holding in the presence of wind disturbances is to increase the gain of the coupling between the aircraft system and the radio beam. However, increase of gain alone causes a loss of overall system stability with the result that any improvement in performance by this manner is extremely limited, in fact the performance is more likely to deteriorate. However, the use of phase advance terms can increase system stability and so allow an increase of coupling gain, and the addition of such terms to the basic glide path control law of a typical autopilot has been investigated on a computer. The terms used have ranged from the time derivative of the glide path signal to combinations of terms obtained from a normal accelerometer and pitch attitude gyros.

In this Report, emphasis is laid on frequency response and statistical response techniques of analysis, since difficulty has been encountered in the past in the prediction of performance from time histories of simulated approaches in the presence of steady or slowly varying wind conditions. The criterion against which performance is measured is the performance

achieved using the simulation of the unmodified control law of the Mark 10B autopilot.

Section 2 discusses the analysis procedures adopted, together with the techniques used for choice of gearings and the difficulties associated with these and past techniques. Section 3 gives a statement of the modifications investigated, followed by a detailed discussion of results in Section 4.

The modified glide path control equations used in this study are listed in the Appendix with the longitudinal equations of motion of the aeroplane (Varsity) and the kinematic and wind equations.

2 ANALYSIS PROCEDURE

In the past there have been marked discrepancies between computer studies of control on the I.L.S. glide path and the results of actual flight trials. For example, work done using the time history record and single discrete wind gusts as disturbances, erroneously predicted a possible gain factor of two or three times the highest practical flight value. For some time these discrepancies were blamed on inaccurate or incomplete simulation of the problem, but recent work has indicated that inadequate methods of assessing the performance achieved on the computer were the main cause of the differences. One difficulty lies in the range dependence of the glide-path signal. The contours of constant error signal are straight lines radiating from the transmitter, so that the error signal received by the aircraft for a given linear displacement from the glide-path beam is greater at short range than at long range from the transmitter. Thus the system gain is low at long range, giving sluggish control, but high at short range, giving a tight control. In this situation it is inadequate to examine the time history of an approach in which the only disturbance is the error at the start, since by the time the system reaches instability because of gain increase, there will be no disturbance to trigger the instability. Similarly the injection of a step disturbance at a given range is inadequate since the effect of this disturbance is critical upon the range at which it is injected, and it is not clear how to choose a range that will be characteristic of the whole approach.

It is clear that the only satisfactory test is to subject the system to random disturbances throughout a series of approaches (as would occur in practice) and to examine statistically the results of such a series. Subsidiary tests could be used to indicate whether the beam capture manoeuvre was satisfactory.

The method of analysis adopted in this Report falls into four distinct stages, of which the first three are additional to previous methods:-

- (i) choice of control gearing values to be used in the modified control laws by a study of stability margins;
- (ii) frequency responses of displacement from the I.L.S. glide path caused by three variables - (a) vertical wind, (b) horizontal wind (c) radio noise;
- (iii) statistical results from simulated approaches in the presence of random horizontal wind variations;
- (iv) a study of approach manoeuvres in the presence of various disturbances, such as the beam join manoeuvre; the effect of rate of descent datum errors, and the effect of wind shears both from head and tail.

Fig.10 shows a block schematic of the computer arrangement.

2.1 Choice of gearing values

Since it is pointless to have a system which gives good performance at long range but is unstable at close range, the gearing values chosen were those which gave as high an overall gearing as was feasible at close range, since high gearings produce tighter control in the presence of wind turbulence. The general method for choice of gearings is illustrated in the following example. With a general control equation of the form:-

$$\theta_c = -K_5 \left(\beta + K_6 \frac{\beta}{D} + K_{101} DH \right)$$

where θ_c = commanded pitch angle,

β = glide path error signal,

H = height of aircraft,

$$D = \frac{d}{dt}$$

K_5, K_6, K_{101} are control gearings,

assume that the required values are those of K_5 and K_{101} , the value of K_6 being invariant. Then K_{101} is fixed at a particular value and K_5 varied until the recovery of the system from a step disturbance is a neutrally damped oscillation. The procedure is repeated at other values of K_{101} and the value of K_5 for neutral stability plotted as a function of K_{101} , thus giving the neutral stability boundary in the K_{101}/K_5 plane. Since the minimum stability occurs at the start of the ATTITUDE phase (100 ft) when the coupling to the

glide path in terms of commanded pitch attitude per foot of displacement from the glide-path beam is a maximum, the above boundary is computed with a fixed height of 100 ft programmed into the computer.

Stability boundaries similar to the above have been plotted for each of the different control equations listed in the Appendix, and the boundaries are shown in Figs. 1 to 7. It was found that in the case of DH damping alone (Fig. 1) the curve reached a maximum, but for most of the other modifications, (Figs. 2 to 5) the curve was a monotonic increasing function of the gearing K_{101} (or K_{102} , etc) up to a point where the rate of pitch command exceeded the limit of $3^\circ/\text{sec}$, when the neutrally damped oscillation suddenly degenerated into a rapidly divergent oscillation at the slightest provocation. The value of K_5 at which this sudden change took place, was not consistent for a given value of K_{101} (or K_{102} , etc) and this area of uncertainty is shown by the hatched areas of Figs. 2 to 5. This effect initially caused concern as to the restrictions it would apply to use of this method of choosing gearing values and an inquiry was made as to its nature.

With no rate limit present the boundary continued smoothly with no discontinuities. Addition of the rate limit alone caused the system to become divergent, but limiting the pitch command amplitude to its standard value of $3\frac{1}{2}^\circ$ contained the oscillation, although it did not damp it out.

While the possibility of such limit cycles might appear unsatisfactory, it was found that with the rate and amplitude limits both present on the pitch command and the finally chosen gearings, an offset of 40 ft from the glide-path at a height of 100 ft was required to initiate the undamped oscillation, and at greater heights the required initial offset was greater than the beam width. This was considered to be a condition most unlikely to be met in practice since both rate and amplitude limits are inserted for reasons of passenger comfort and safety.

Flight experience has shown that the optimum value of the terminal gearing is about half that value which gives instability. The choice was therefore nominally half the maximum value of K_5 attainable on the stability boundary plots. Unfortunately, due to the effects of the limit cycles referred to above, this was not always a clear choice. Hence the final choice was based on the judgement of the computer operator with the empirical criterion of half the instability value kept in mind. The values chosen are marked on Figs. 1 to 5.

2.2 Frequency responses

The frequency responses measured are defined as the ratio of an output parameter of the system, say displacement, to an input parameter, say wind

variation, at a particular frequency. Since a frequency response is only valid for a linear system, the convergence characteristics of the glide path had to be ignored and a linear sensitivity assumed. For the reasons stated in Section 2.1, the sensitivity chosen was that corresponding to a height of 100 ft.

Three different frequency responses were made for each modified control law and the results obtained were compared with the results from the other analysis techniques. Measurements were taken to establish the relationship between the displacement of the aircraft from the glide-path to:-

- (a) noise on the I.L.S. radio signal,
- (b) horizontal wind,
- (c) vertical wind

at frequencies in the range 0.01 to 1 c/s.

2.3 Statistical results

In order to verify that frequency responses measured at a fixed height were representative of performance during the approach, a set of approaches was simulated for each modified system in the presence of random horizontal wind gusts, and the aircraft displacement and velocity at right angles to the beam centre-line at the start of ATTITUDE were measured and analysed. From these measurements, means and standard deviations were calculated for each set of approaches and the results compared with those of the frequency response analysis.

The wind input used in the statistical measurements was produced from a random white-noise generator. The output of the generator had a Gaussian distribution of amplitude with a power spectrum which was sensibly flat from 0.04 cps to 10 cps. Since all computing was done in accelerated time (time constants decreased by a factor of ten) the effective spectrum was flat from 0.004 cps to 1 cps.

The spectrum was shaped by passing the output through a filter of the form $\frac{1}{(1 + L/V_g D)}$ where L is a characteristic turbulence dimension, here = 1000 ft, V_g is the aircraft airspeed = 186 ft/sec. This gave a filter of $\frac{1}{1 + 5.4 D}$ giving a cut-off at 6 dB per octave from 0.03 cps. The transfer function characteristic of the filter is plotted in Fig.9.

2.4 Time history

The time histories were intended to give an overall qualitative picture of the approach from beam capture to start of ATTITUDE in the presence of wind shear, discrete gusts or in no wind. The purpose of these time histories was not to differentiate between the systems but to ensure that the other methods of system analysis had not overlooked important aspects of performance.

3 MODIFICATIONS TO THE CONTROL LAWS

The first requirement of any modification was to improve the beam holding in the presence of turbulence without decreasing the stability at low height. The second requirement was that the modification should be a simple one to engineer. Since displacement from the beam is preceded by velocity and acceleration, then information about either velocity or acceleration normal to the beam will provide advance information on beam displacement errors. Because of the consideration of engineering simplicity it was decided to investigate the use of a signal derived from an accelerometer positioned in the aircraft on the centre of gravity so as to provide a measure of acceleration along the z-axis of the aircraft. Velocity along the z-axis was obtained by integration of the accelerometer signal. The information derived from the accelerometer was used in conjunction with that from a pitch rate gyro, to produce the effect of displacing the accelerometer from the centre of gravity. The complete control equations used are listed in the Appendix, but in brief the modifications investigated were the addition of:

(a) $f(DH)$

(b) $f(DH + D\theta)$

(c) $f(DH + D^2H)$

(d) $f(D^2H)$

(e) $f(D^2H + D^2\theta)$

to the basic equation $\theta_c = -K_5 \left(\beta + \frac{K_6 \beta}{D} \right)$.

Included in the simulation of the accelerometer was a filter of time constant 0.2 sec, to represent the filter which would be needed in practice to attenuate mechanical vibration of the accelerometer.

The possibility of adding a simple beam-rate term to the basic equation was considered, but this was rejected for a number of reasons. Fig.6, the plot of the neutral stability boundary for beam-rate damping shows that a significant

increase of overall gearing is only possible if the lag on the signal is less than about 0.1 sec. Unfortunately, with such a small lag the amount of noise required to cause the demanded pitch rate to exceed the limit of $3^\circ/\text{sec}$ is less than 14 microamps at frequencies between 1.0 and 2.0 c/s, see Fig.8. This is less than that allowed by I.C.A.O. so that glide path beams within the specification would be likely to cause rate limiting. Further to this, the shape of the stability boundary is so sharply peaked that even assuming no limit problems, the practical difficulty of producing the required gearing values would be considerable. Another possible addition to the basic equation that was considered was that of a simple pitch-rate term, $D\theta$. However this gave no improvement in stability as is shown in Fig.8 and it was rejected.

4 DETAILED DISCUSSION OF THE RESULTS

4.1 Frequency responses

4.1.1 Response of the aircraft to beam signal

The criterion against which to compare the beam response caused by the various modifications to the control law was taken to be the beam response of the unmodified system using the basic control law. The requirements for beam response are (a) unity gain from DC up to about 1 c/s and (b) a sharp cut-off at about 1 c/s to attenuate the effects of high frequency noise. Since the closed-loop characteristic equation of the aircraft/autopilot system contains complex poles, such requirements are not met since resonances produce greater than unity gain^{4,5}. Hence the requirements for the modified system are that they increase bandwidth without increasing the resonant gain. Fig.11 to 14 show the effects of the various modifications.

It is clear that the addition of D^2H only or $(D^2H + D^2\theta)$ each produce unacceptable resonant gains at 0.11 c/s (Fig.13), indicating a poor beam holding in the presence of disturbances at this frequency. The addition of terms DH , $(DH + D\theta)$ and $(D^2H + DH)$ all give a wider bandwidth with a lower resonance, although the presence of the pitch-rate term appears to sharpen the peak slightly.

4.1.2 Response to horizontal wind

The frequency response measured was the amplitude of displacement produced by a wind whose velocity varied sinusoidally, and was plotted as feet displacement per foot per second of horizontal wind (Figs.15 to 18). Ideally it is required that the aircraft response to wind is zero at all frequencies, but Fig.15 shows that in the case of the basic unmodified system this is certainly

not so. At gust frequencies around 0.1 c/s, an amplitude of ± 5 kts will produce deviations from glide-path of about ± 12 ft at a height of 100 ft. The spectrum is such that between periods of 50 seconds and 8 seconds, a 5 kt variation on the wind produces greater than 7 ft deviation from the glide slope, and since 100 ft height is the start of ATTITUDE, this deviation will carry through to produce a touchdown range error of about 150 ft.

The modifications involving D^2H and $(D^2H + D^2\theta)$, see Fig.17, cause an unacceptable resonance at 0.11 c/s, although the response away from the peak is an improvement over that obtained with the unmodified control law (Fig.15). A similar resonance was obtained on the responses due to beam signals. In the case of the modifications with DH , $(DH + D\theta)$ and $(D^2H + DH)$ (Figs.16 and 18) the curves have moved bodily to higher frequencies relative to the basic response curve, and the gains decreased. This has the effect of greatly improving the responses at lower frequencies while giving a slight degradation at frequencies above about 0.2 c/s, i.e. about 5 sec period gusts. Fig.9 shows that at 0.2 c/s the amplitude of the horizontal wind is attenuated to about 0.14 that at zero frequency so that a slight degradation of performance at this frequency is unimportant. The greatest reduction in horizontal wind response was produced by the $(D^2H + DH)$ modification (Fig.18), the reduction varying from a factor of ten at 0.003 c/s to a factor of 5 at 0.1 c/s. Above this frequency the improvement becomes less until at 0.2 c/s the response curve of the basic system crosses that of the modified control law.

4.1.3 Response to vertical wind

The response of the system to vertical winds (Figs.19 to 22) was measured as a function of the height error caused by variation of the vertical wind speed. The results as given by the vertical wind responses are identical to those of the horizontal wind case in that D^2H and $(D^2H + D^2\theta)$ give exaggerated maxima while the least response is from $(D^2H + DH)$. The latter modification gives a reduction factor of about 2.7 at frequencies less than about 0.15 c/s when its response curve again converges with and crosses that of the basic system. With the basic system the maximum displacement from glide path is 2.8 ft/ft/sec for 0.1 c/s gusts. The greatest displacement with $(D^2H + DH)$ occurs at a frequency of 0.185 c/s when the displacement is 1.3 ft/ft/sec. The modifications with D^2H and $(D^2H + D^2\theta)$ give a degraded response, the displacement produced by 1 ft/sec gusts being 4 ft for $(D^2H + D^2\theta)$ at 0.11 c/s.

4.2 Statistical treatment of response to random horizontal wind

In order to verify the predictions given by the frequency responses, simulated approaches were made for each modification state in the presence of random horizontal wind with an rms velocity of 4 ft/sec equivalent to a mean wind speed of about 12 kts and a simple statistical analysis made of the displacement and velocities perpendicular to the glide slope at the start of ATTITUDE. Twenty-five simulated approaches were made with each control law, and each approach was stopped at a height of 100 ft and the above parameters recorded from a digital voltmeter. The means and standard deviations of the displacements and velocities were then calculated, and from these an estimate of touchdown range error due to random wind variations was made.

Previous work² has shown that the touchdown range error produced by a vertical velocity error of 1 ft/sec at the start of ATTITUDE is about 175 ft for a nominal rate of descent of 10 ft/sec (a 3° glide path and an approach speed of 186 ft/sec gives a nominal rate of 9.74 ft/sec). Assuming such a range error due to velocity error, and assuming that displacement errors are carried through geometrically to give 19.1 ft/ft of beam error for a 3° glide slope Table 1 gives the standard deviation of touchdown range caused by horizontal wind for the different control laws, and Fig. 23 gives examples of the approaches in the presence of random horizontal wind of rms velocity 4 ft/sec.

Table 1

Additional control function	Velocity error (Dh) (ft/sec)	Displacement error (h) (ft)	Touchdown error in ft due to		Total touchdown error (ft)
			Dh	h	
None	0.94	3.44	164	36	176
DH	0.54	1.53	94	29	98
(DH + D θ)	0.39	0.94	67	18	70
(DH + D 2 H)	0.41	1.09	72	21	75
D 2 H	0.75	4.4	132	84	156
(D 2 H + D 2 θ)	0.71	2.34	124	45	132

All the above numbers represent standard deviations.

Fig. 24 illustrates in diagrammatic form the difference in range error produced by the different modifications.

4.3 Time history

Simulated beam captures and approaches were made from a height of 2000 ft for each control law investigated in three different sets of wind conditions:-

- (i) zero wind,
- (ii) tailwind shear (i.e. tailwind whose speed is dropping with height),
- (iii) headwind shear with a horizontal gust of 5 ft/sec at 300 ft height.

In each instance it was considered that if the beam joining manoeuvre for a particular control law was not grossly different from that of the others, then small differences in behaviour were only important at close range, i.e. at heights below 500 ft.

4.3.1 Approaches in zero wind

As seen from Fig.25 all of the modifications to the control law produce improvements in the beam joining in zero wind conditions. Normal aircraft instruments would indicate that the aircraft was established if the error from the beam was less than about 15 microamps; this would mean that all of the systems were established immediately. Hence all of the modifications produced satisfactory beam joining in zero wind conditions.

4.3.2 Approaches in the presence of a tailwind shear

The wind simulation was a tailwind of 50 ft/sec at a height of 2000 ft falling linearly to 20 ft/sec at ground level, and Fig.26 shows that if the criterion of 15 microamps is taken, then those systems using either no extra term of DH damping only are not established until below 500 ft height. The other systems all reach the 15 microamp criterion by a height of about 1200 ft although the system using (DH + D θ) damping only just remains inside the 15 microamp limit after the second crossing of the beam centre-line.

4.3.3 Approaches in the presence of a headwind shear and a gust

Fig.27 shows the combined effect of a wind shear and a horizontal wind gust from ahead, the gust being a step of 5 ft/sec injected at a height of 300 ft. The wind simulated for the headwind shear was a headwind of 50 ft/sec at a height of 2000 ft, falling linearly to 20 ft/sec at ground level.

All of the systems achieved good beam joining performances, even the unmodified system resulting in the glide path error signal being less than 15 microamps by a height of 1400 ft. Those control systems using ($D^2H + D^2\theta$), ($D^2H + DH$) and D^2H only were within this limit immediately and kept to within

5 microamps after the third beam crossing. This is much better performance than that achieved in a tailwind shear, but it should be noted that the change in performance is entirely due to the sign of the wind direction at 2000 ft height rather than to the sign of the shear itself. Even in zero wind the aircraft overshoots the glide path and a tailwind makes the overshoot worse, whilst a headwind reduces it. Nevertheless since the general tendency is for wind strength to decrease as height is reduced, it is considered that the method of simulating wind shear represents a disturbance likely to be encountered in practice.

The response of the systems to a step gust followed approximately the results predicted by the frequency responses except for the response of the systems using $(D^2H + D^2\theta)$ and D^2H damping, whose gust responses were predicted to be worse than those of the basic system. It must be realised, however, that the gust was injected at a height of 300 ft to allow time for a complete recovery while the frequency responses were measured at a height of 100 ft. Frequency responses measured at heights greater than 100 ft show that the very sharp resonance in the responses of the system using D^2H and $(D^2H + D^2\theta)$ falls off rapidly with increase in height (see Fig.16) and frequency responses measured at 300 ft agree with the results of the gust injection at 300 ft.

4.4 Effect of an error on the datum rate-of-descent in the control laws using DH

The use of a rate-of-descent term for damping in the control equation requires that the velocity signal derived from the accelerometer be biased, so that zero signal is obtained when the aircraft is descending at a rate appropriate to the glide-path angle and approach speed of the aircraft.

Since beam angles will vary between about 2.5° and 3.5° and aircraft ground speed will vary according to wind conditions, approaches were recorded for the control law modifications involving DH, $(D^2H + DH)$ and $(DH + D\theta)$ in various wind conditions, with errors on the datum rate of descent of about $\pm 30\%$, equivalent to beam angles of $3^\circ \pm 1^\circ$. This is also equivalent to an actual beam angle of $3^\circ \pm 0.5^\circ$ plus a head or tailwind of 28 ft/sec (16.5 kts).

The sign convention used is as follows:- if the datum rate of descent set into the pitch computer is less than that required for the glide-path angle, then the error is defined as negative. Hence an error of -30% on a glide path of nominal rate of descent 9.75 ft/sec means that the datum is set for a rate of descent of 6.82 ft/sec. Figs.28 to 30 show the effect, for a glide-path with a nominal rate of descent of 9.75 ft/sec, of an error of ± 3 ft/sec.

Fig.28 shows the effects of such errors in the absence of any outside disturbance, other than the beam join manoeuvre, and comparison with Figs.25 and 26 indicate the similarity of the effect of wind shears from head and tail with no datum error. This is only to be expected since both effectively produce ground speed errors if the airspeed is assumed to be constant. When a 30% error on the datum rate-of-descent is coupled with either a head or tailwind shear, Figs.29 and 30, the effect of the error is added algebraically to the shear so that either an improvement or a degradation in the beam join manoeuvre may be achieved. In both cases the effect of the error is only evident during the first part of the approach, there being little difference in the path flown with perfect datum and with a datum error below a height of about 600 ft.

Even with as large an error as 30% on the datum, the performance in glide-path capture using DH , $(DH + D\theta)$ or $(D^2H + DH)$ in the control law is comparable to that of the basic control law as used at present in the Varsity/Mk.10B system.

5 CONCLUSIONS

The purpose of this study was to investigate the possibility of improving the aircraft's performance on the I.L.S. glide path and so reduce the effect of wind variations on the scatter of the touchdown point. The results obtained confirm that such an improvement is possible for the simulated system using the additional terms $(DH + D\theta)$ or $(D^2H + DH)$ in the control law.

While these terms do not produce the best beam capture in the presence of windshears, it is considered that the greater improvement in the presence of wind gusts, coupled to the higher probability of encountering wind gusts than that of encountering wind shears, recommends the use of either $(DH + D\theta)$ or $(D^2H + DH)$.

The use of either of these terms has been shown to reduce the standard deviation of touchdown range due to horizontal wind turbulence in the ratio 5:2 and even allowing for practical deficiencies, a considerable reduction should be achievable.

A flight programme is now in hand to investigate the practical validity of the conclusions.

Appendix

GENERAL EQUATIONS USED IN THE SIMULATION

Control law modifications

The basic control law as used at present in the B.L.E.U. system is:-

$$1 \quad \theta_c = \frac{-K_5}{(1 + 0.2 D)(1 + 0.5 D)} \left\{ \beta + K_6 \frac{\beta}{D} \right\}$$

The modifications to the control law produced:-

$$2 \quad \theta_c = \frac{-K_5}{(1 + 0.2 D)(1 + 0.5 D)} \left\{ \beta + K_6 \frac{\beta}{D} + \frac{K_{101} D^H}{(1 + 0.2 D)} \right\}$$

$$3 \quad \theta_c = \frac{-K_5}{(1 + 0.2 D)(1 + 0.5 D)} \left\{ \beta + K_6 \frac{\beta}{D} + \frac{K_{101}}{(1 + 0.2 D)} [D^H + K_{105} D^0] \right\}$$

$$4 \quad \theta_c = \frac{-K_5}{(1 + 0.2 D)(1 + 0.5 D)} \left\{ \beta + K_6 \frac{\beta}{D} + \frac{K_{102} D^2 H}{(1 + 0.2 D)} \right\}$$

$$5 \quad \theta_c = \frac{-K_5}{(1 + 0.2 D)(1 + 0.5 D)} \left\{ \beta + K_6 \frac{\beta}{D} + \frac{K_{102}}{(1 + 0.2 D)} [D^2 H + K_{103} D^2 \theta] \right\}$$

$$6 \quad \theta_c = \frac{-K_5}{(1 + 0.2 D)(1 + 0.5 D)} \left\{ \beta + K_6 \frac{\beta}{D} + \frac{K_{101} D^H + K_{102} D^2 H}{(1 + 0.2 D)} \right\} .$$

The value of K_6 was fixed at $1/30 \text{ sec}^{-1}$ for all of the equations.

The values of the other coefficients, optimised for each equation, were:-

Equation (1) $K_5 = 0.02^\circ/\mu\text{a}$

Equation (2) $K_5 = 0.03^\circ/\mu\text{a}, K_{101} = 7 \mu\text{a}/\text{ft}/\text{sec}$

Equation (3) $K_5 = 0.04^\circ/\mu\text{a}, K_{101} = 7 \mu\text{a}/\text{ft}/\text{sec}, K_{105} = 1.0 \text{ ft}/\text{sec}/\text{sec}$

Equation (4) $K_5 = 0.03^\circ/\mu\text{a}, K_{102} = 3 \mu\text{a}/\text{ft}/\text{sec}^2$

Equation (5) $K_5 = 0.04^\circ/\mu\text{a}, K_{102} = 5 \mu\text{a}/\text{ft}/\text{sec}^2, K_{103} = 0.175 \text{ ft}/\text{sec}^2/\text{sec}^2$

Equation (6) $K_5 = 0.05^\circ/\mu\text{a}, K_{101} = 7 \mu\text{a}/\text{ft}/\text{sec}, K_{102} = 3 \mu\text{a}/\text{ft}/\text{sec}^2$

Aerodynamic equations

After substitution for the aerodynamic derivatives of the Varsity aircraft in the approach configuration, the equations are:-

$$\text{Equation (7)} \quad \frac{du}{dt} + 0.0224 (u + u_w) - 0.338 + 0.562 \theta = \frac{T}{m}$$

$$\text{Equation (8)} \quad 0.1068 (u + u_w) + 0.938 \alpha + \frac{d\alpha}{dt} + \frac{d\alpha_w}{dt} - \frac{d\theta}{dt} + 0.1234 \eta = 0$$

$$\text{Equation (9)} \quad 0.474 \frac{d\alpha}{dt} + 2.2 \alpha + \frac{d^2\theta}{dt^2} + 1.481 \frac{d\theta}{dt} + 6.524 \eta = 0$$

Equations of motion

$$\text{Equation (10)} \quad \frac{dH}{dt} = \frac{V_e (\theta - \alpha)}{57.3}$$

$$\text{Equation (11)} \quad \frac{dh}{dt} = \frac{dH}{dt} + \frac{(V_e - W)s}{57.3}$$

$$\text{Equation (12)} \quad R = R_0 - [V_e - W + (u + u_w)] t$$

$$\text{Equation (13)} \quad \beta = \frac{s R_F}{R} h$$

Wind equations

$$\text{Equation (14)} \quad \text{Shear : } W = W_2 + (W_1 - W_2) \frac{H}{H_0}$$

$$\text{Equation (15)} \quad \text{Longitudinal wind : } u_w = W - W_1$$

$$\text{Equation (16)} \quad \text{Vertical wind : } \alpha_w = \frac{W_e}{V_e}$$

Control equations

$$\text{Equation (17)} \quad \text{Basic autopilot : } G_1 \frac{(1 + 0.3 D)}{(1 + 0.1 D)^2} \left[(\theta - \theta_c) + G_2 \frac{P}{D} \right]$$

$$\text{Equation (18)} \quad P = \left[(\theta - \theta_c) + \frac{57.3}{g} \frac{du}{dt} \right]$$

$$\text{Equation (19)} \quad \text{Locking unit : } \theta_c = \frac{-K_5 \left[\beta + K_6 \frac{P}{D} + f(DH, D^2H, D\theta, D^2\theta) \right]}{(1 + 0.2 D)(1 + 0.5 D)}$$

$$\text{Equation (20)} \quad \text{Autothrottle : } \frac{T}{m} = \frac{-T_1}{(1 + D)(1 + 0.5 D)} \left[(u + u_w) + T_2 \frac{(u + u_w)}{D} \right] + \frac{T_3 \theta}{(1 + D)(1 + 0.5 D)}$$

Values of parameters

- $\epsilon = +3^\circ$
- $R_0 = 38200 \text{ ft}$
- $W_1 = 50 \text{ ft/sec}$
- $W_2 = 20 \text{ ft/sec}$
- $V_e = 186 \text{ ft/sec}$
- $H_0 = 2000 \text{ ft}$
- $sR_F = 18000 \text{ millivolts}$
- $G_1 = 2.0 \text{ degrees/degree}$
- $G_2 = 1/15 \text{ sec}^{-1}$
- $T_1 = 0.1 \text{ (equivalent to about 180 lb/kt for Varsity of mass 1055 slugs)}$
- $T_2 = 0.05 \text{ sec}^{-1}$
- $T_3 = 0.35 \text{ (= 590 lb/degree)}$

SYMBOLS

- θ_0 = commanded pitch angle in degrees
 u = forward airspeed change in ft/sec
 $\alpha = \frac{W}{V_0}$ in degrees, where:-
 w = aircraft airspeed along its z axis
 V_0 = datum airspeed
 θ = pitch angle in degrees, relative to the earth's horizontal
 η = elevator angle in degrees
 H = height of aircraft above ground
 H_0 = initial height of aircraft above ground
 h = perpendicular height of aircraft above or below the glide slope
 R = range from glide path aerial
 R_0 = starting range of aircraft from glide path aerial
 W = wind speed at a height H
 W_1 = wind speed at a height H_0
 W_2 = wind speed at ground level
 G_1, G_2, K_5, K_6 are autopilot parameters
 T_1, T_2, T_3 are autothrottle parameters

REFERENCES

<u>No.</u>	<u>Author</u>	<u>Title, etc.</u>
1	I.C.A.O.	International standards and recommended practices. Aeronautical Telecommunications Annex 10 to the Convention of International Civil Aviation
2	N. H. Hughes G. P. Lazenby	A flight experiment to determine the effects of flare entry conditions on automatic landing performance. R.A.E. Tech. Report TR.65283
3	J. K. Brozek	The relationship between the discrete gust and power spectrum presentations of atmospheric turbulence, with a suggested model of low altitude turbulence R & M 3216
4	Thaler Brown	Servo-mechanism analysis. McGraw Hill Electrical & Electronic Engineering Series
5	John G. Truxal	Control System Synthesis. McGraw Hill Electrical & Electronic Engineering Series

BLANK PAGE

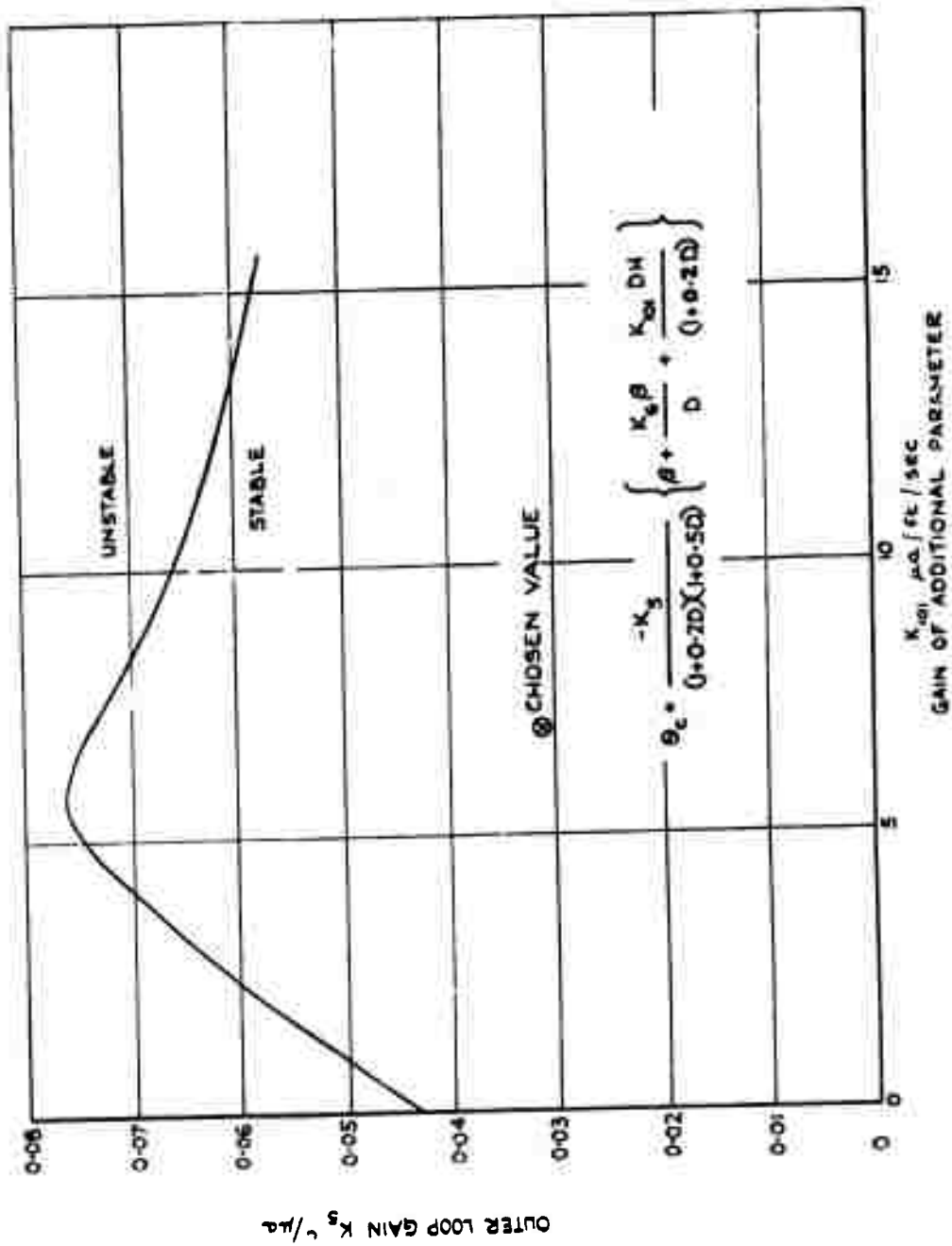


FIG. 1 NEUTRAL STABILITY BOUNDARY FOR D H DAMPING

Fig.2

601-900022

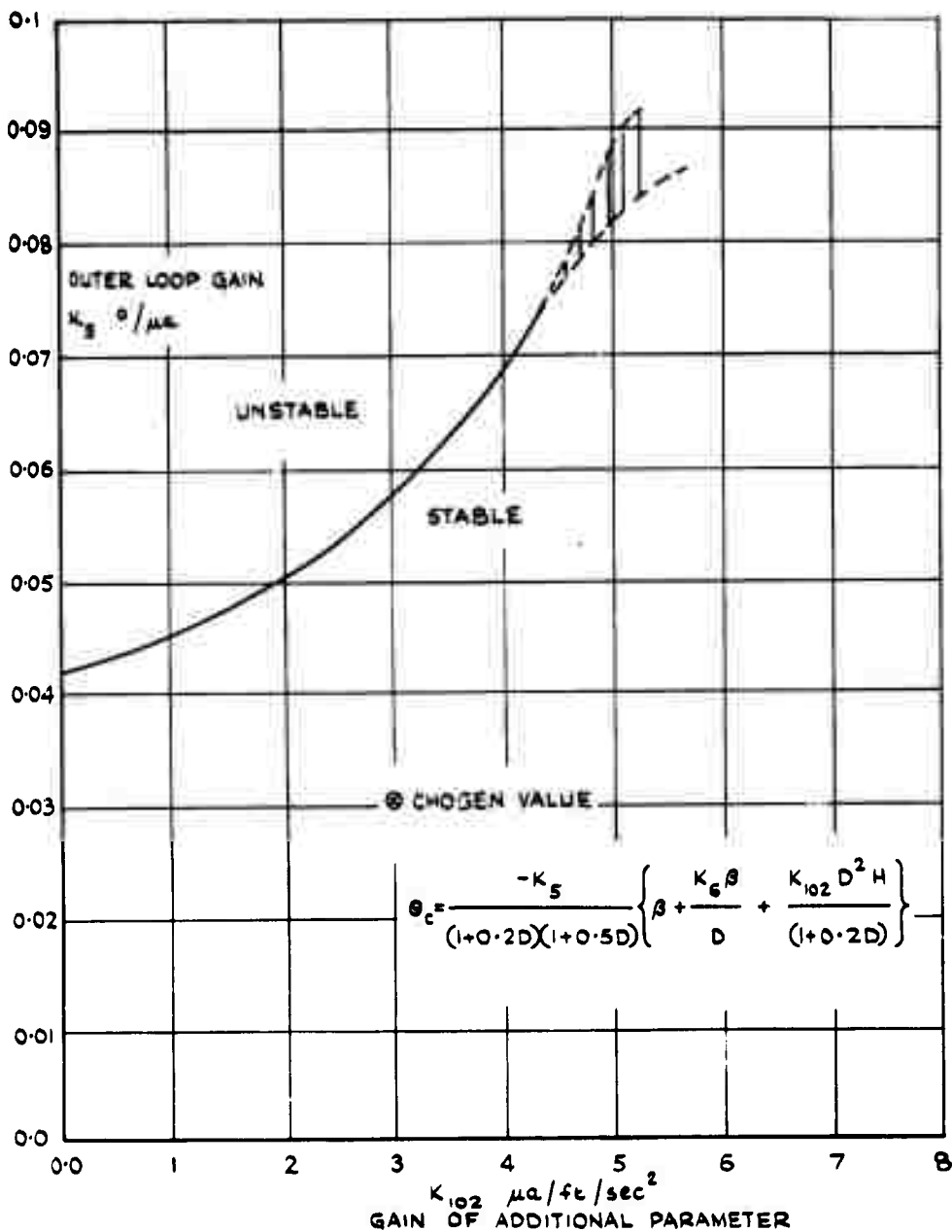


FIG. 2 NEUTRAL STABILITY BOUNDARY FOR
 $D^2 H$ DAMPING

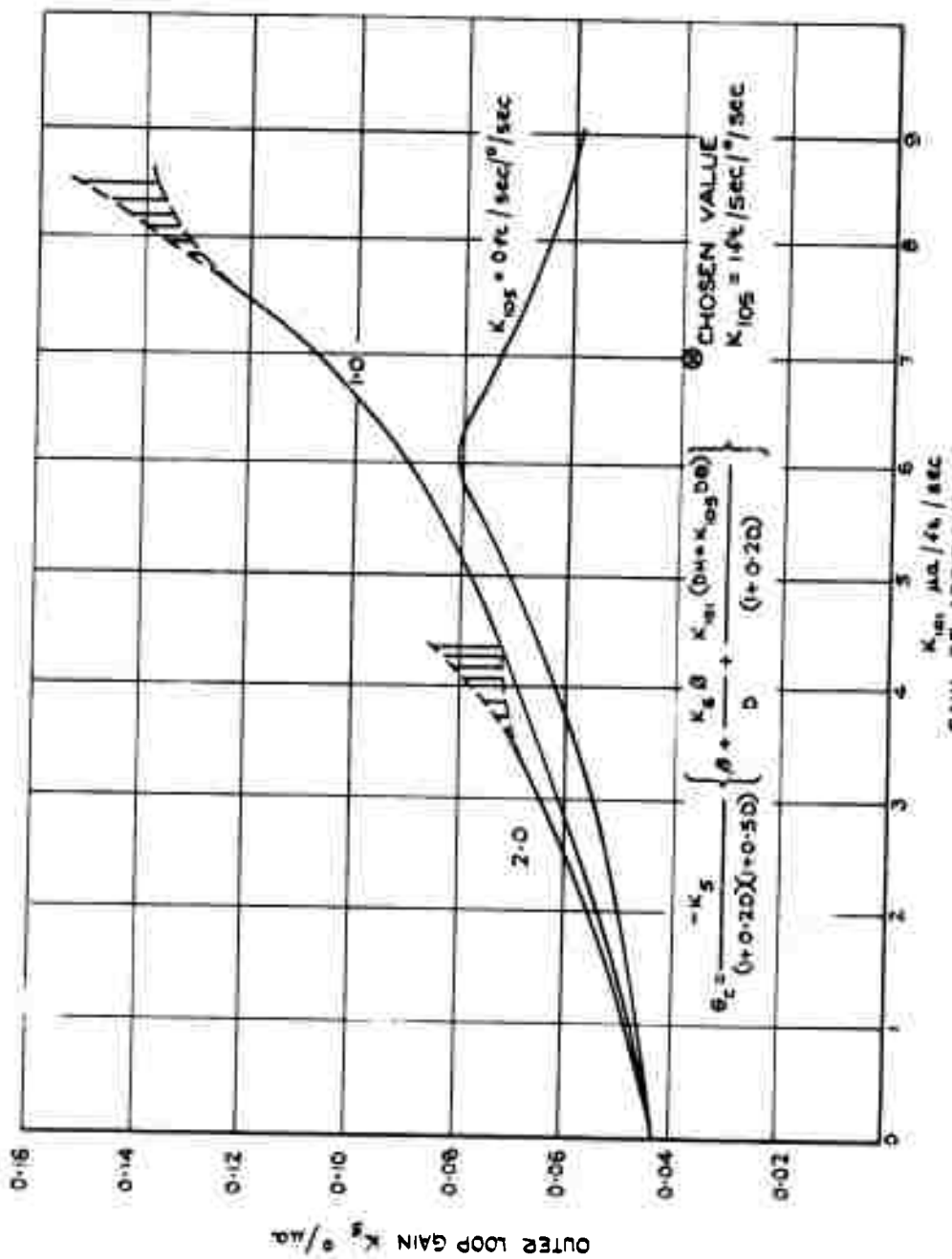


FIG. 3 NEUTRAL STABILITY BOUNDARY FOR (DH + DΘ) DAMPING

Fig.4

601 - 900024

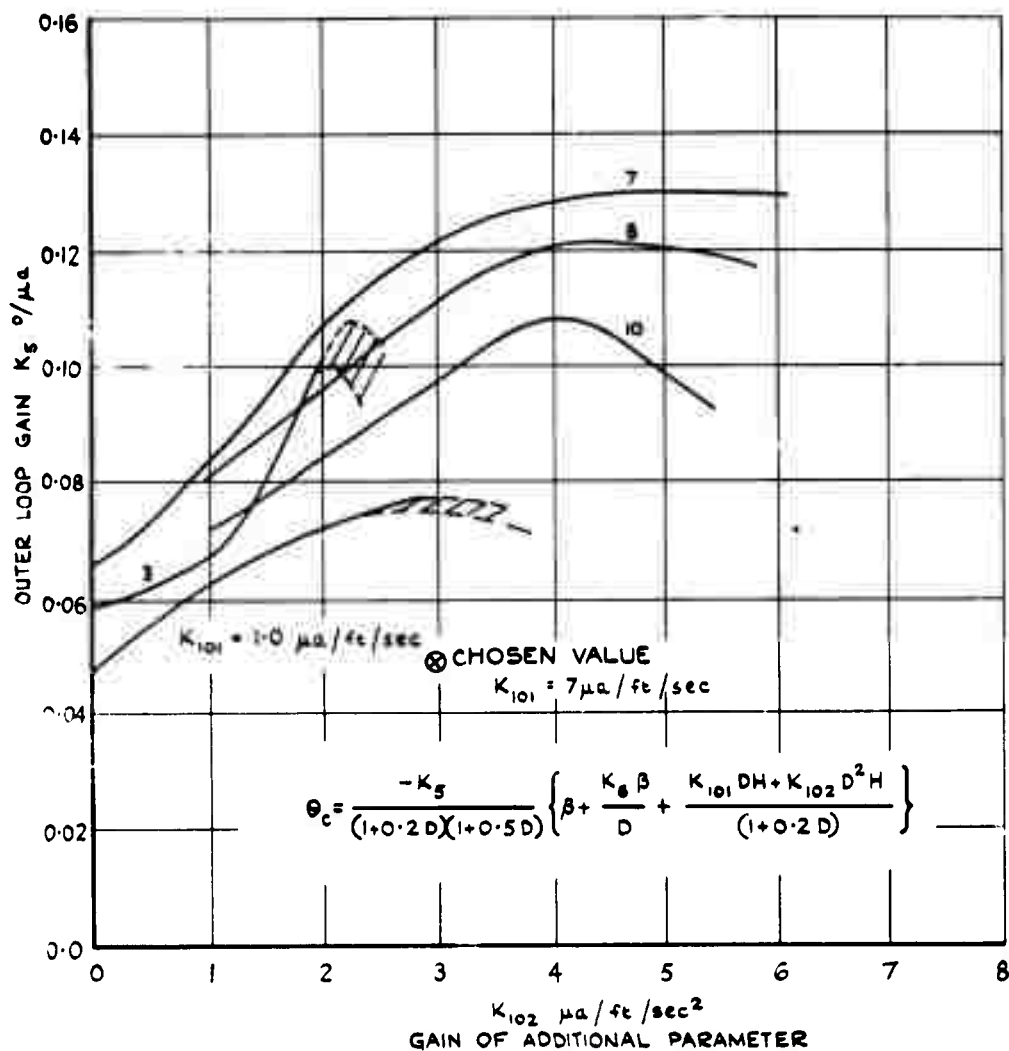


FIG. 4 NEUTRAL STABILITY BOUNDARY FOR
 $(D^2H + DH)$ DAMPING

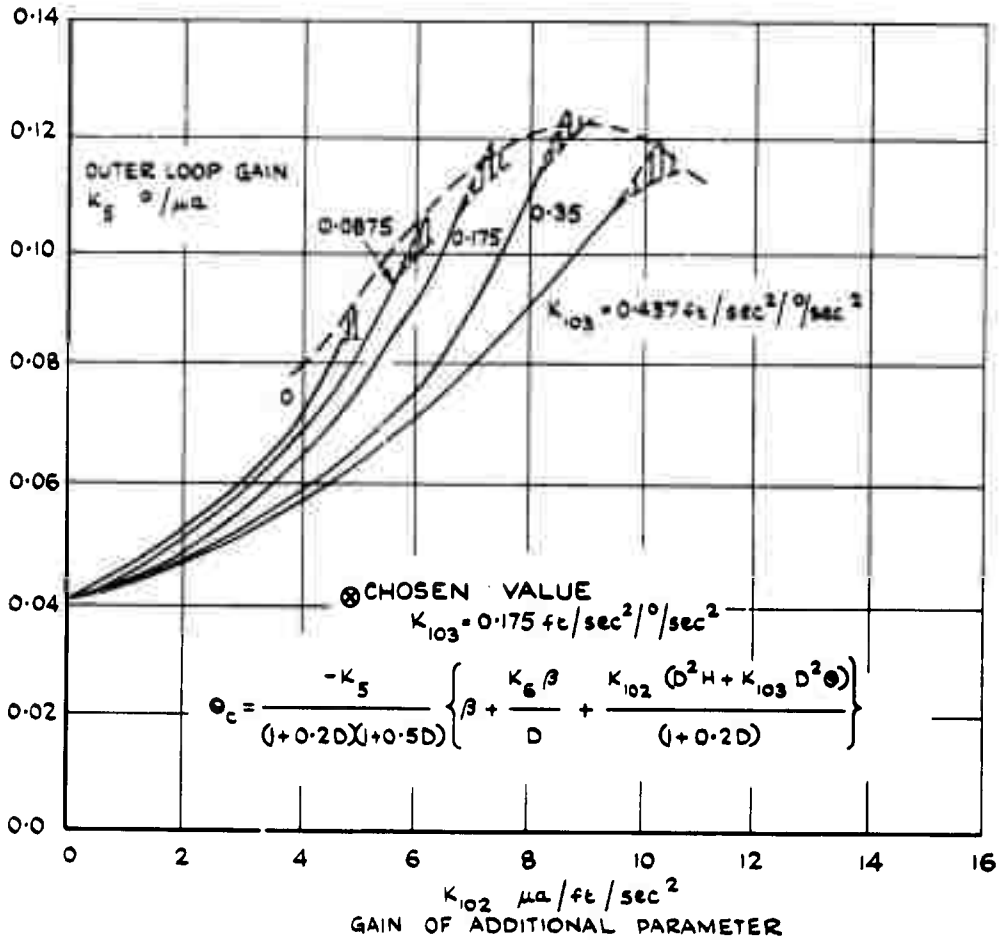
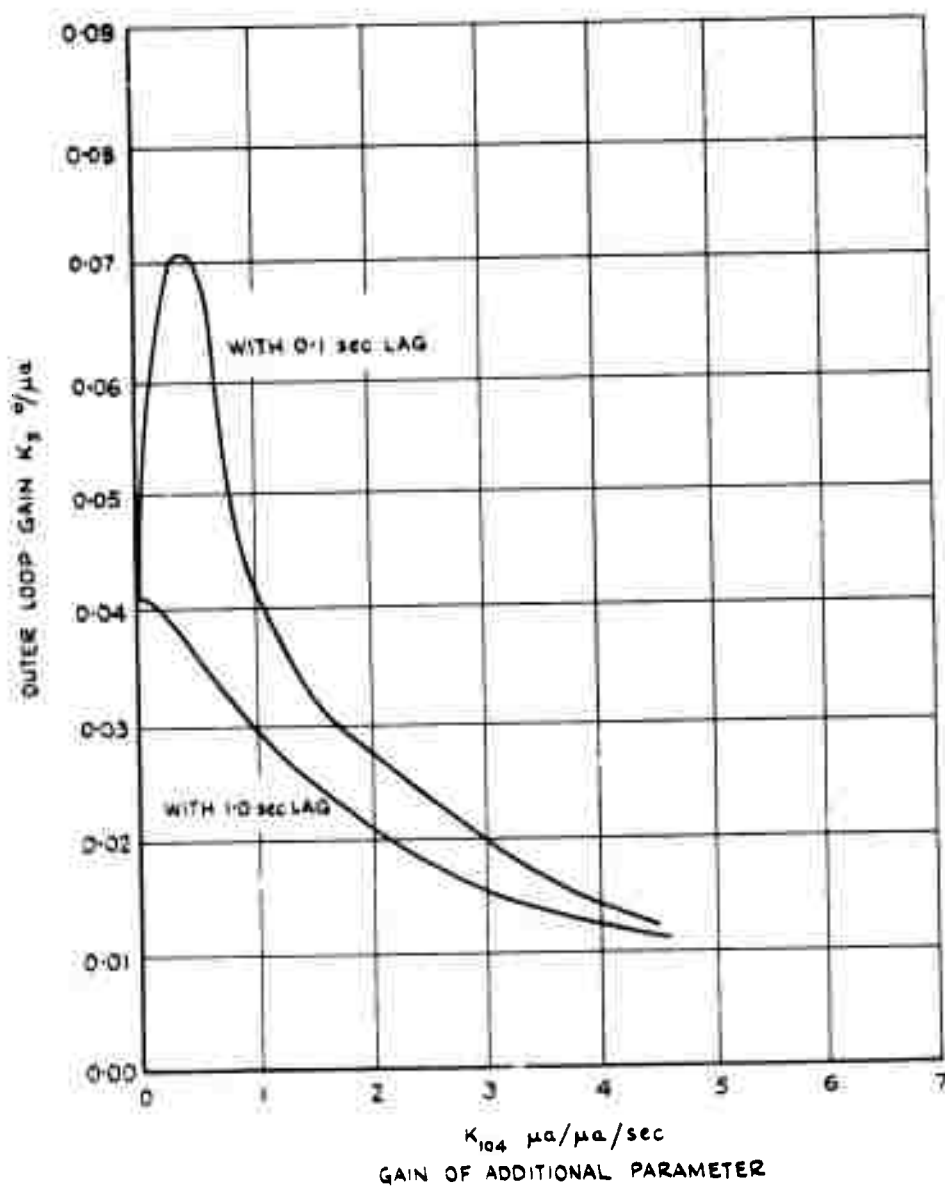


FIG. 5 NEUTRAL STABILITY BOUNDARY FOR
($D^2 H + D^2 \theta$) DAMPING

Fig.6

601-900026

FIG. 6 NEUTRAL STABILITY BOUNDARY FOR $D\beta$ DAMPING

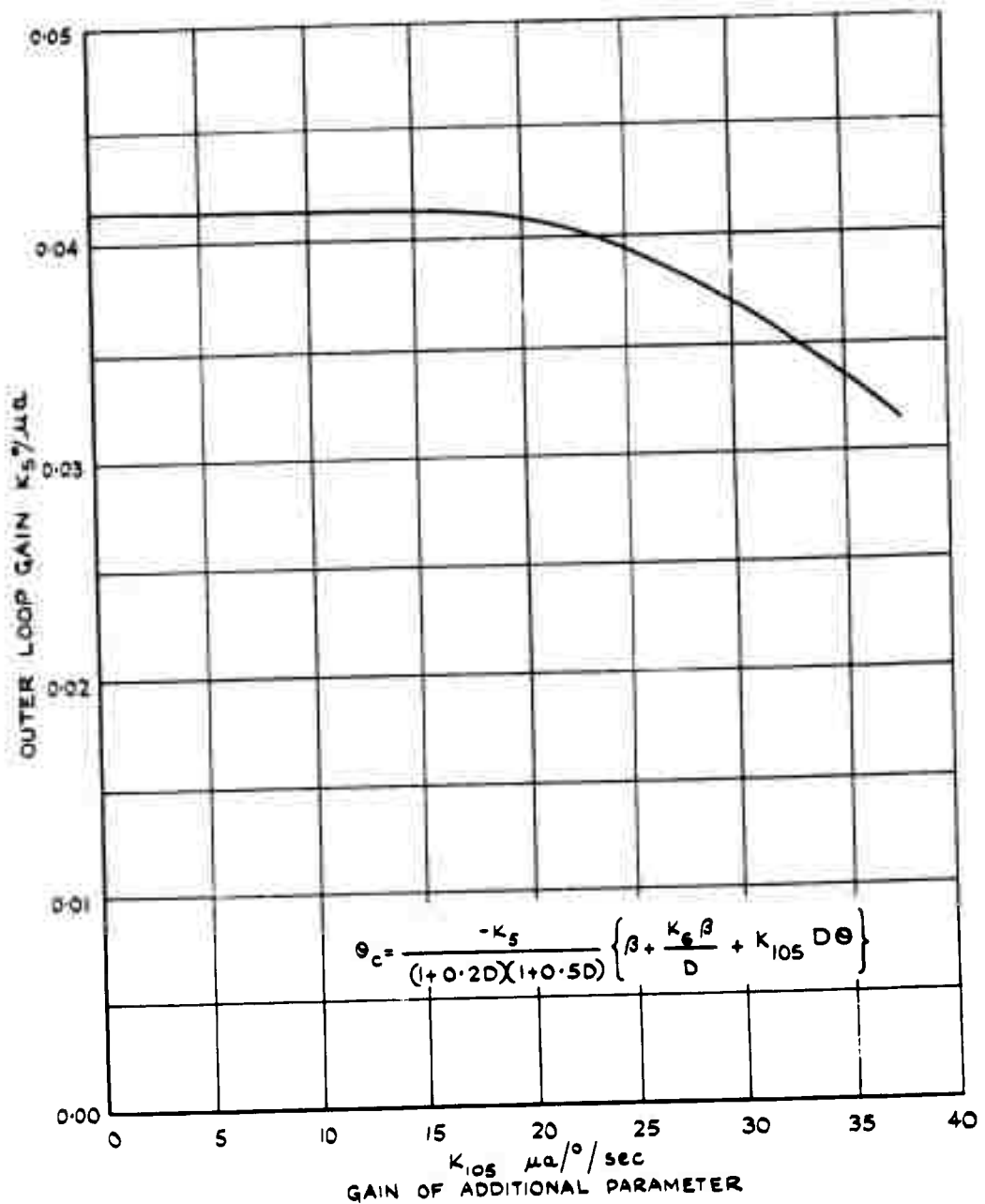


FIG.7 NEUTRAL STABILITY BOUNDARY FOR
Dθ DAMPING

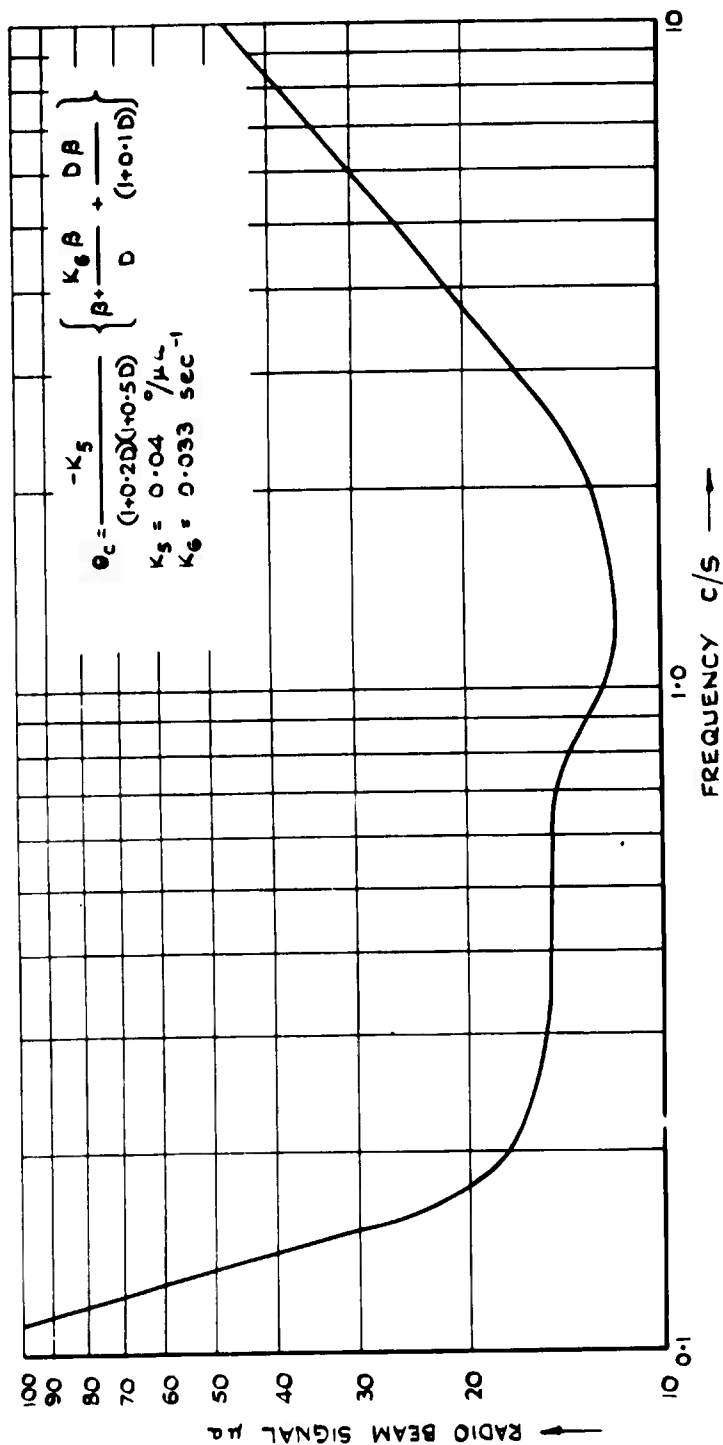


FIG.8 NOISE INPUT REQUIRED TO EXCEED THE 3°/SEC PITCH RATE LIMIT WITH DB DAMPING

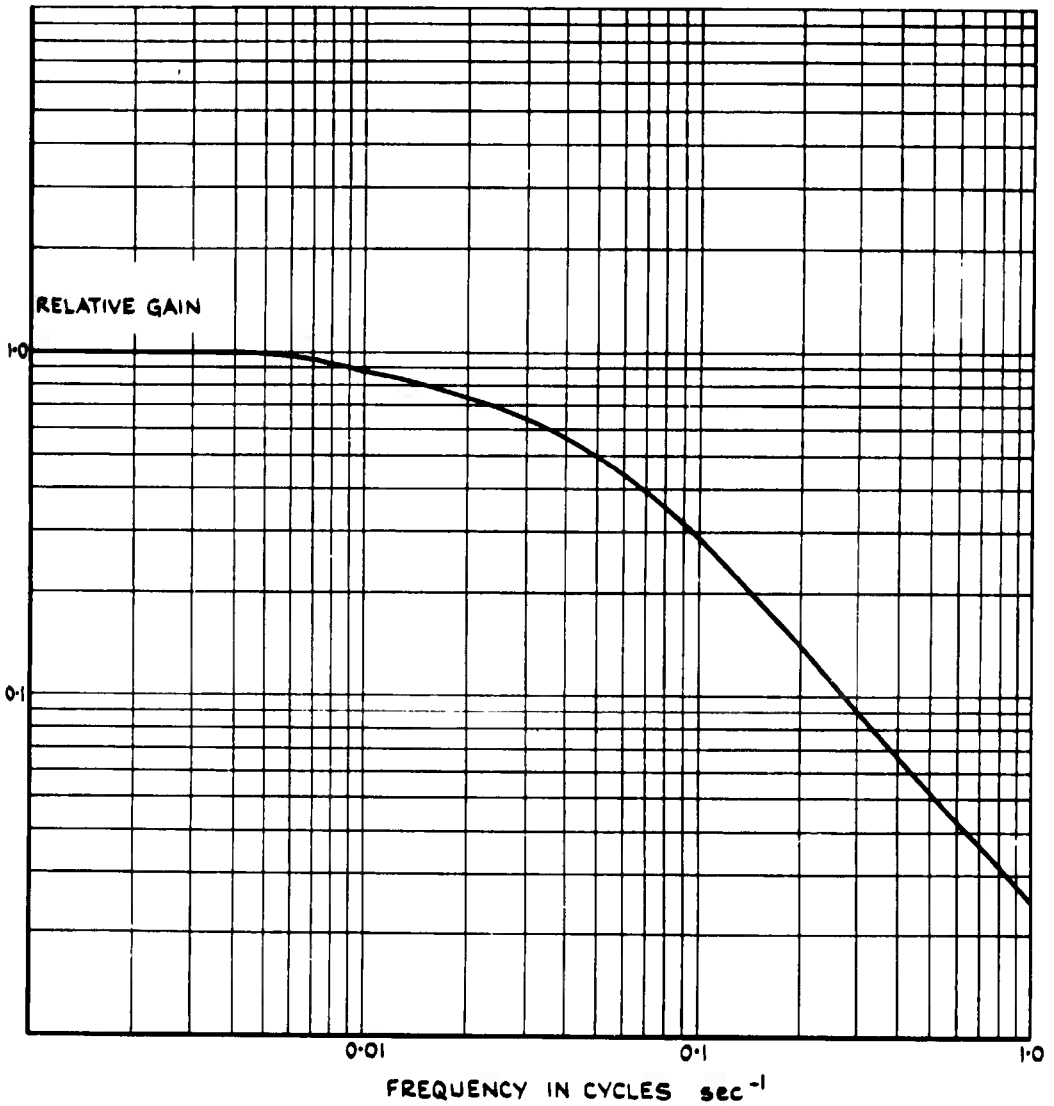


FIG.9 CHARACTERISTIC OF THE SIMPLE FILTER

$$\frac{V_{OUT}}{V_{IN}} = \frac{1}{1 + 5.4D}$$

Fig.10

601 - 9000 30

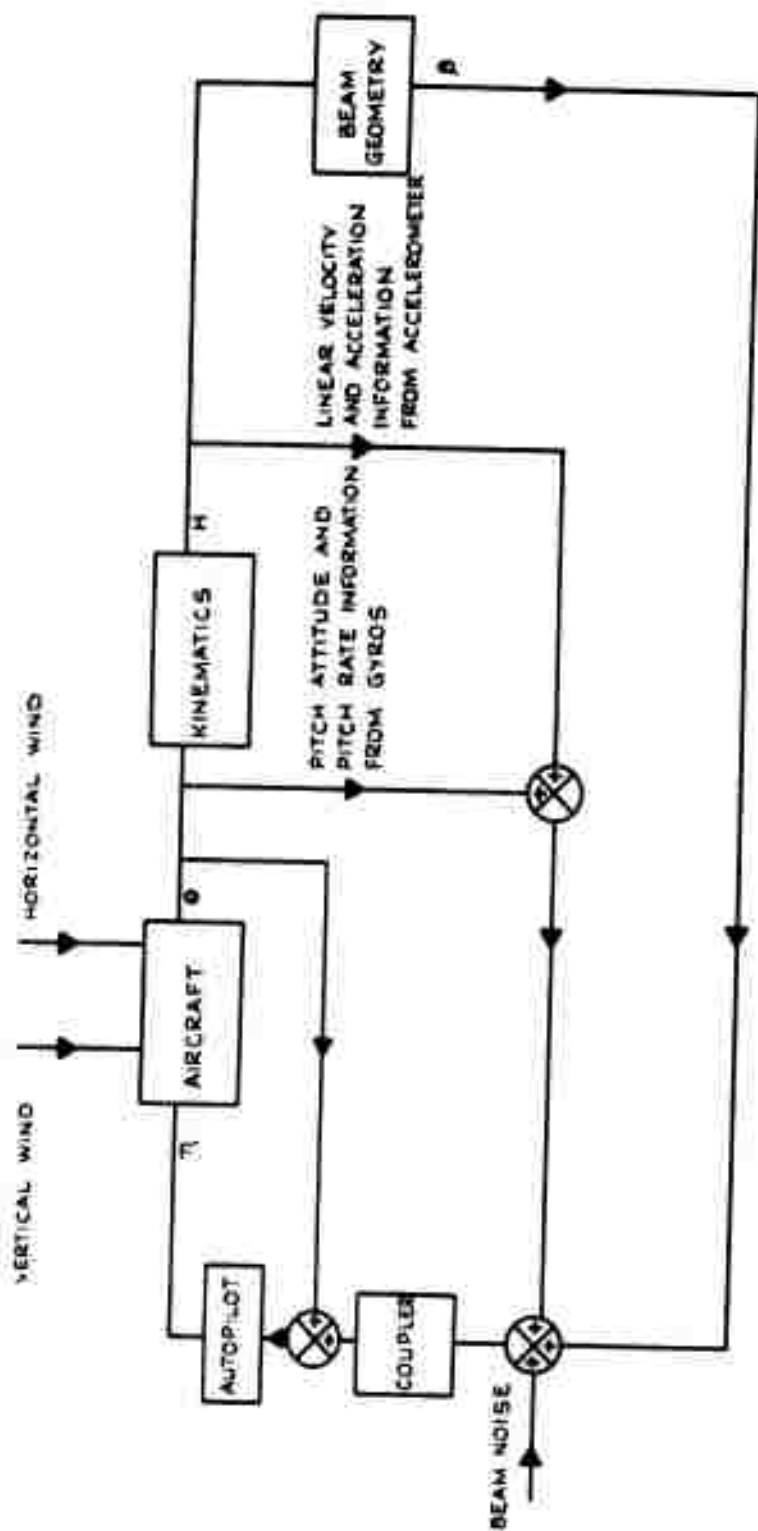


FIG.10 BLOCK DIAGRAM OF THE SIMULATED AIRCRAFT/AUTOPILOT/COUPLER COMBINATION

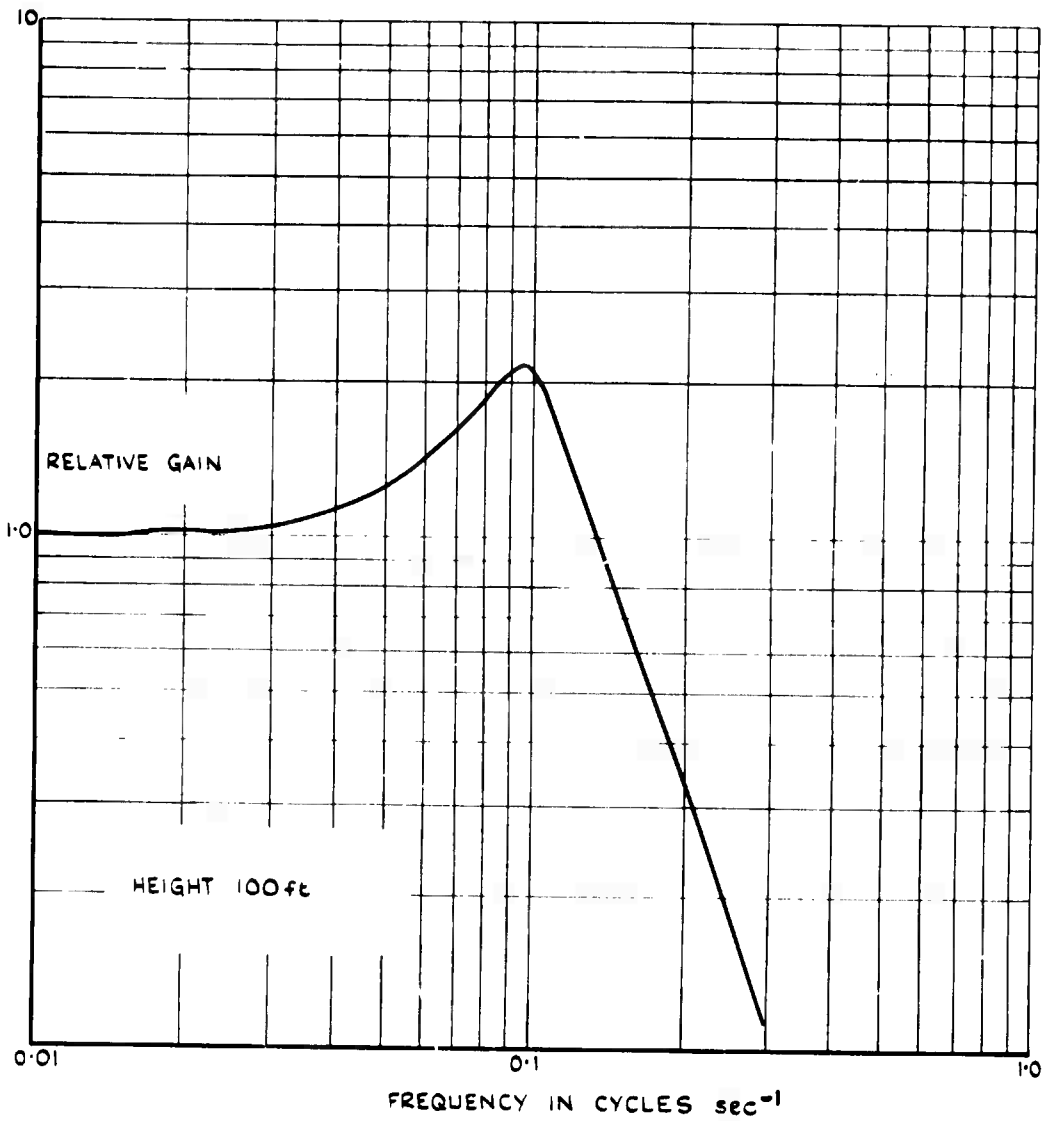


FIG.11 FREQUENCY RESPONSE TO RADIO SIGNAL
OF THE BASIC CONTROL SYSTEM

Fig.12

601-900032

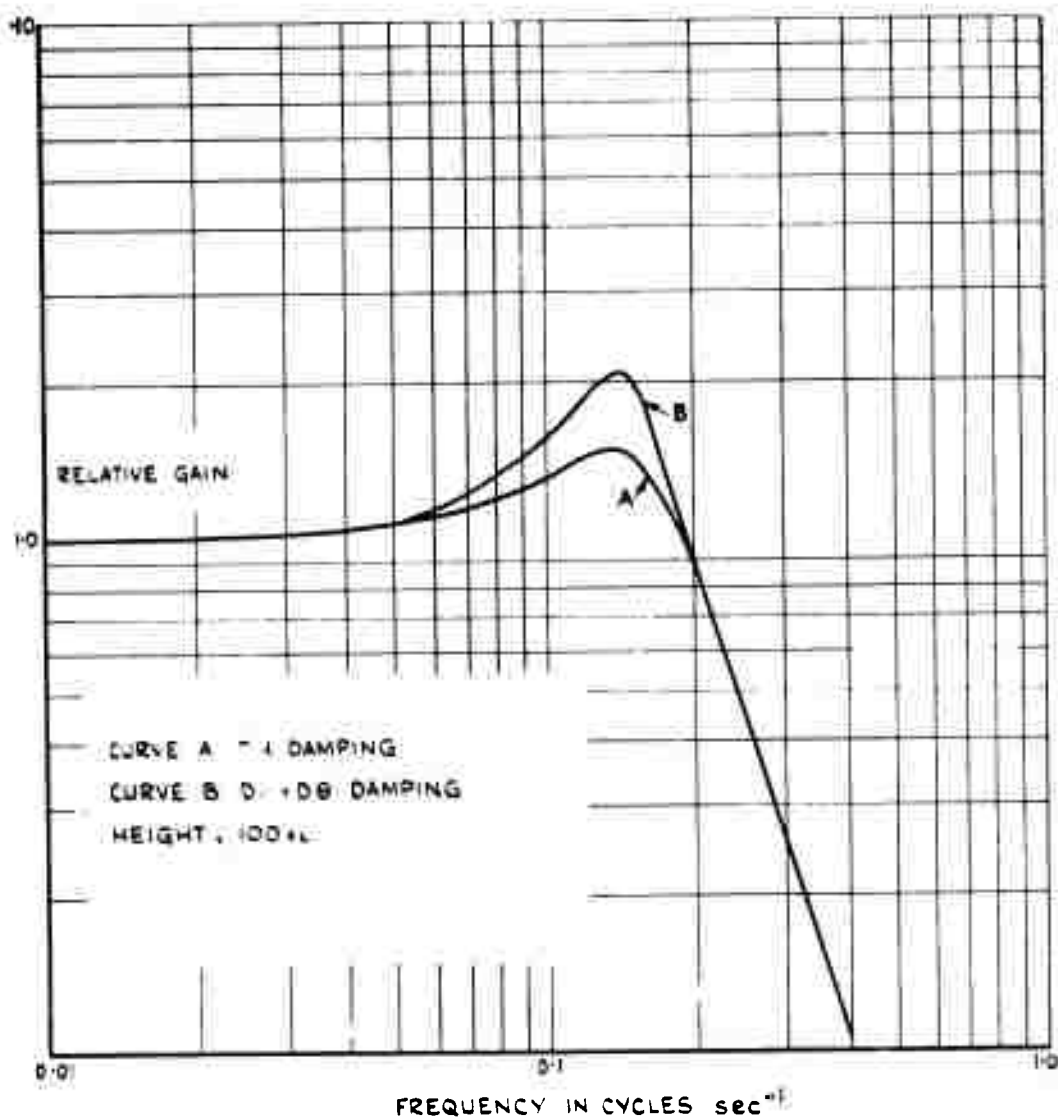


FIG. 12 FREQUENCY RESPONSE TO RADIO SIGNAL

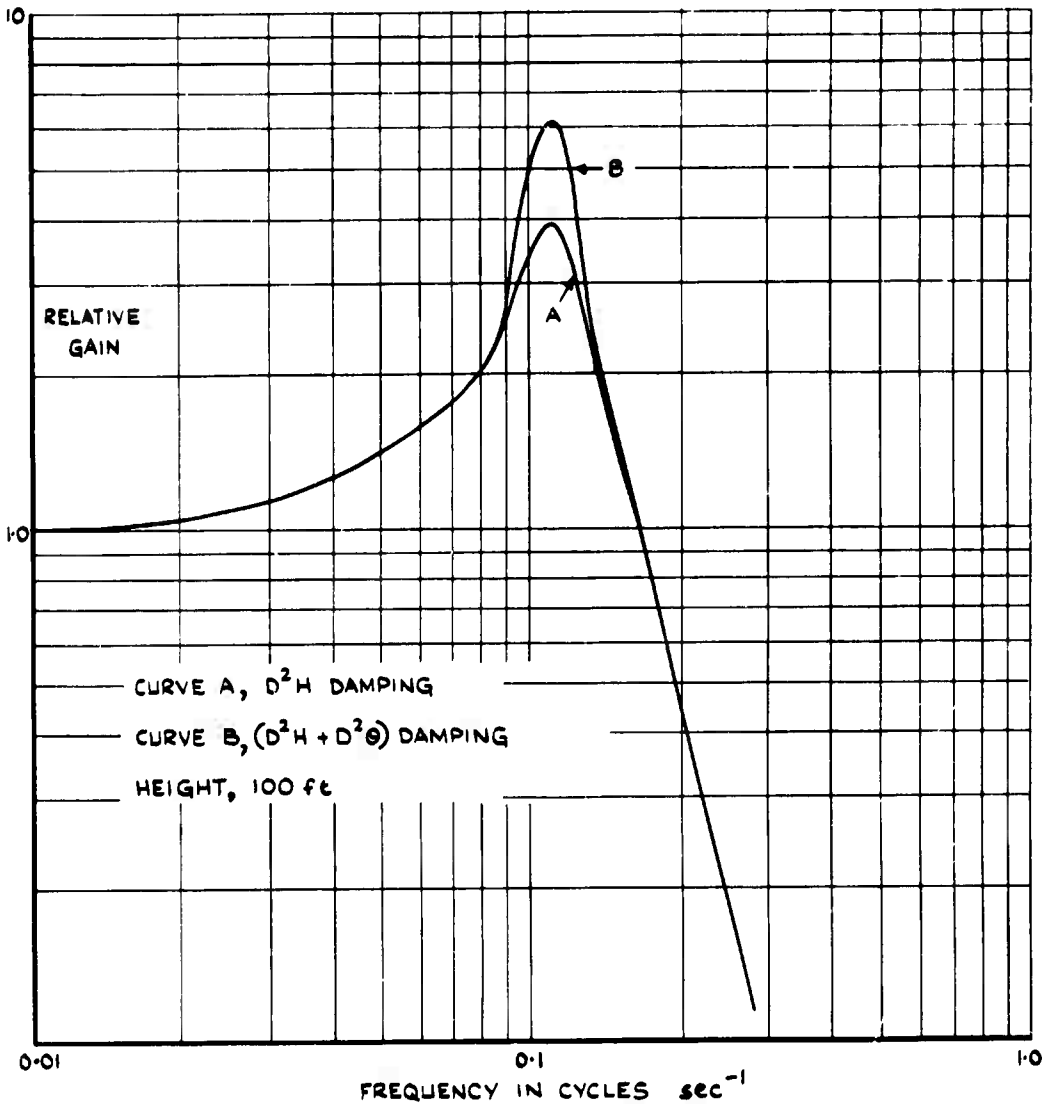


FIG.13 FREQUENCY RESPONSE TO RADIO SIGNAL

Fig.14

601-900034

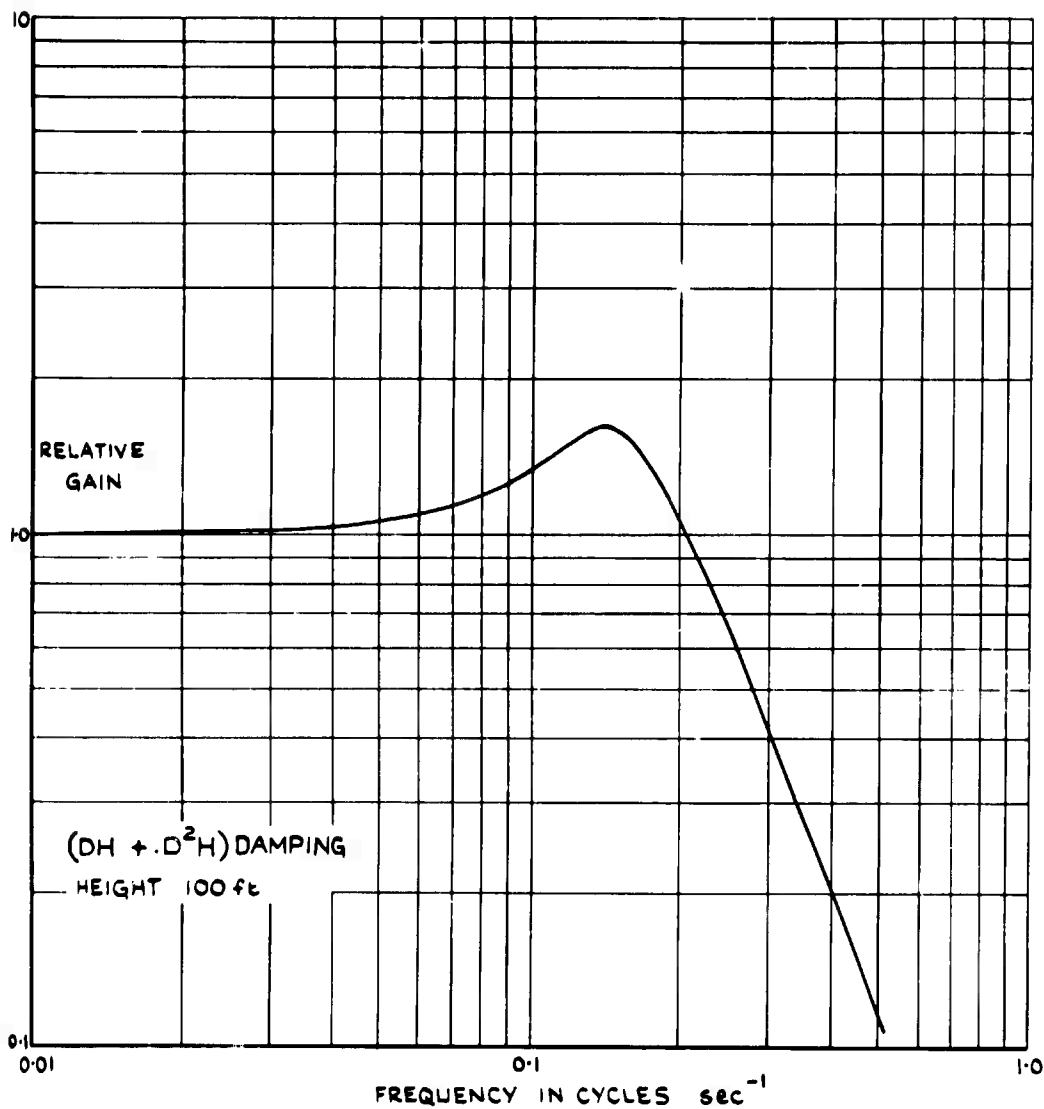


FIG.14 FREQUENCY RESPONSE TO RADIO SIGNAL

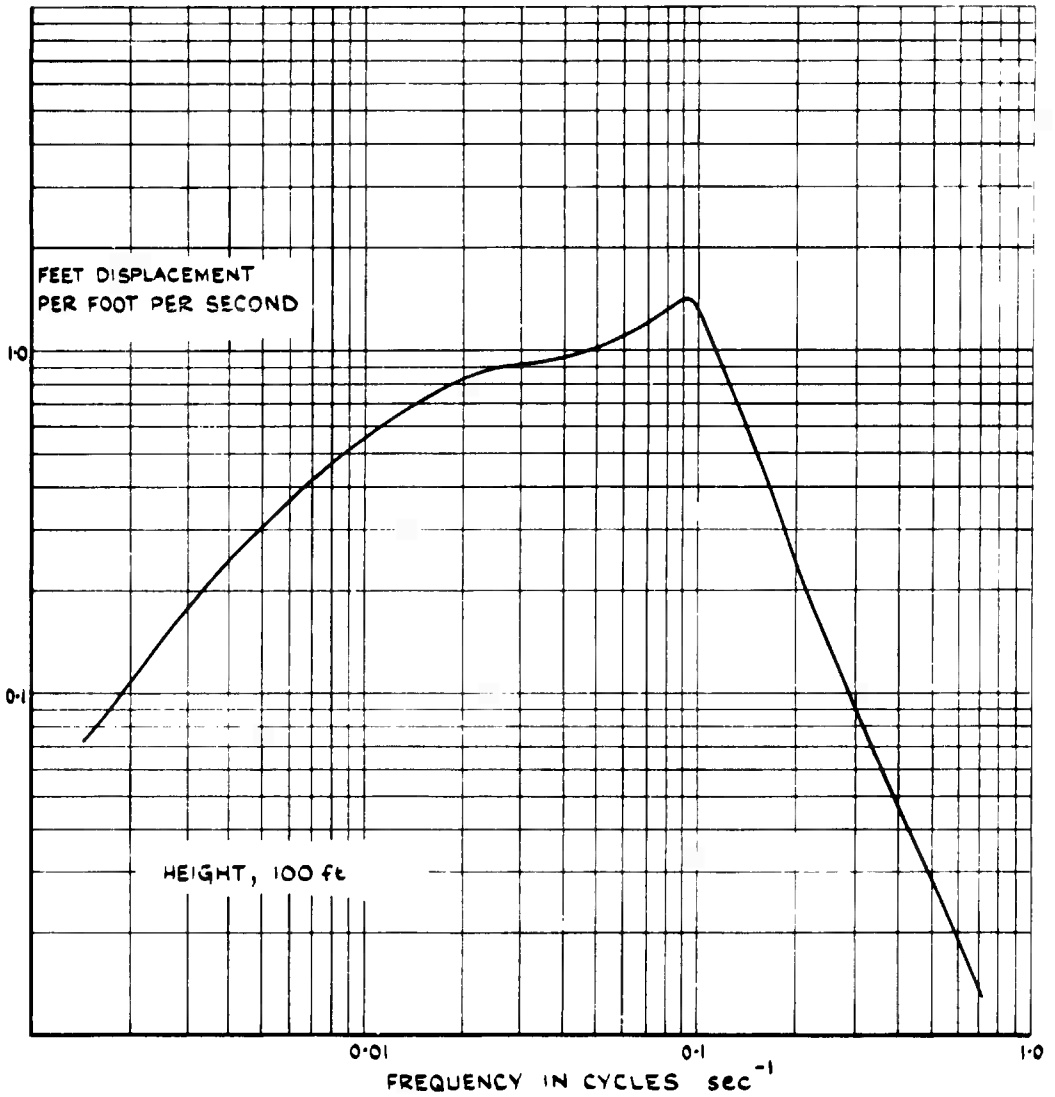


FIG. 15 FREQUENCY RESPONSE
TO HORIZONTAL WIND VARIATIONS OF THE BASIC SYSTEM

Fig.16

601 900036

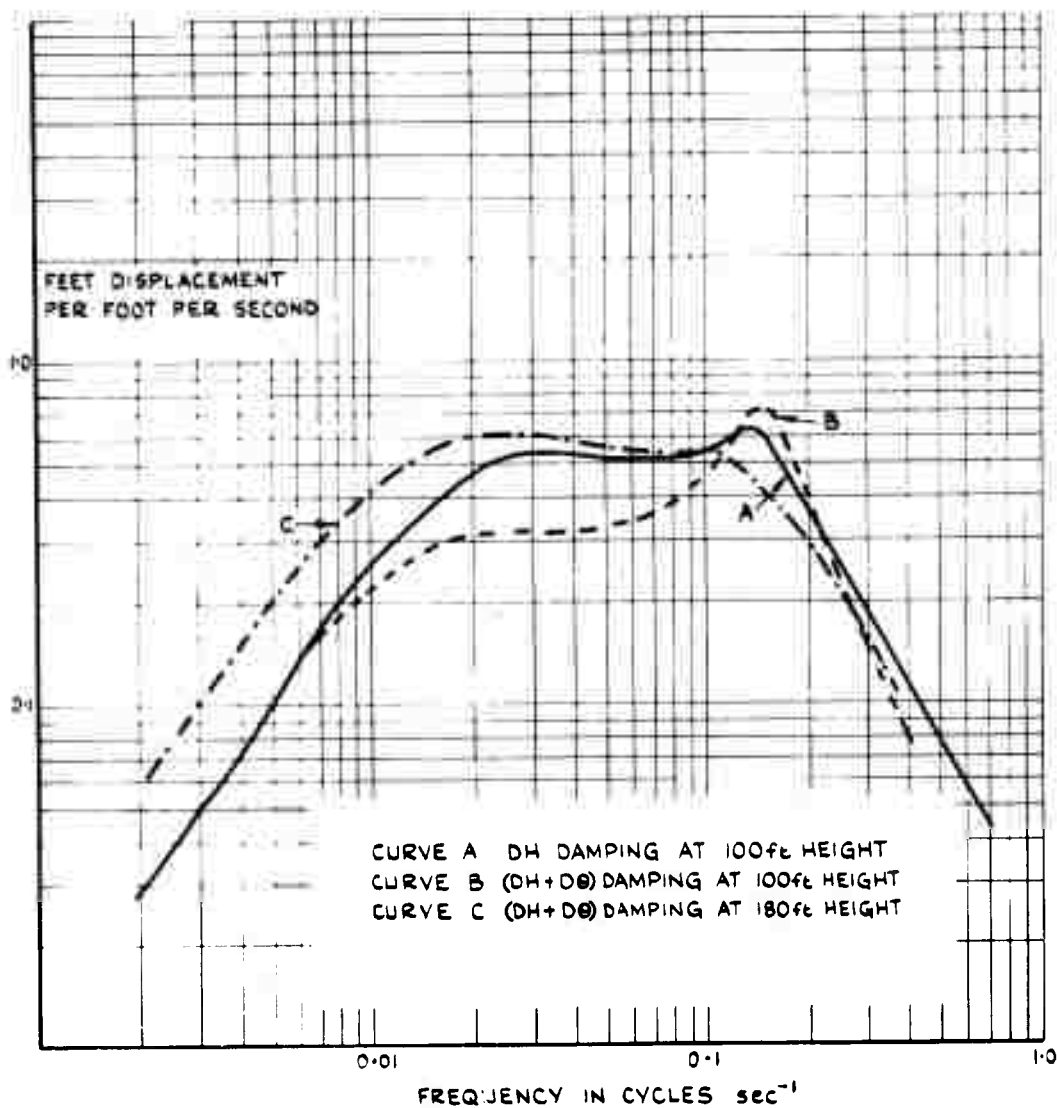


FIG.16 FREQUENCY RESPONSE TO HORIZONTAL
WIND VARIATIONS

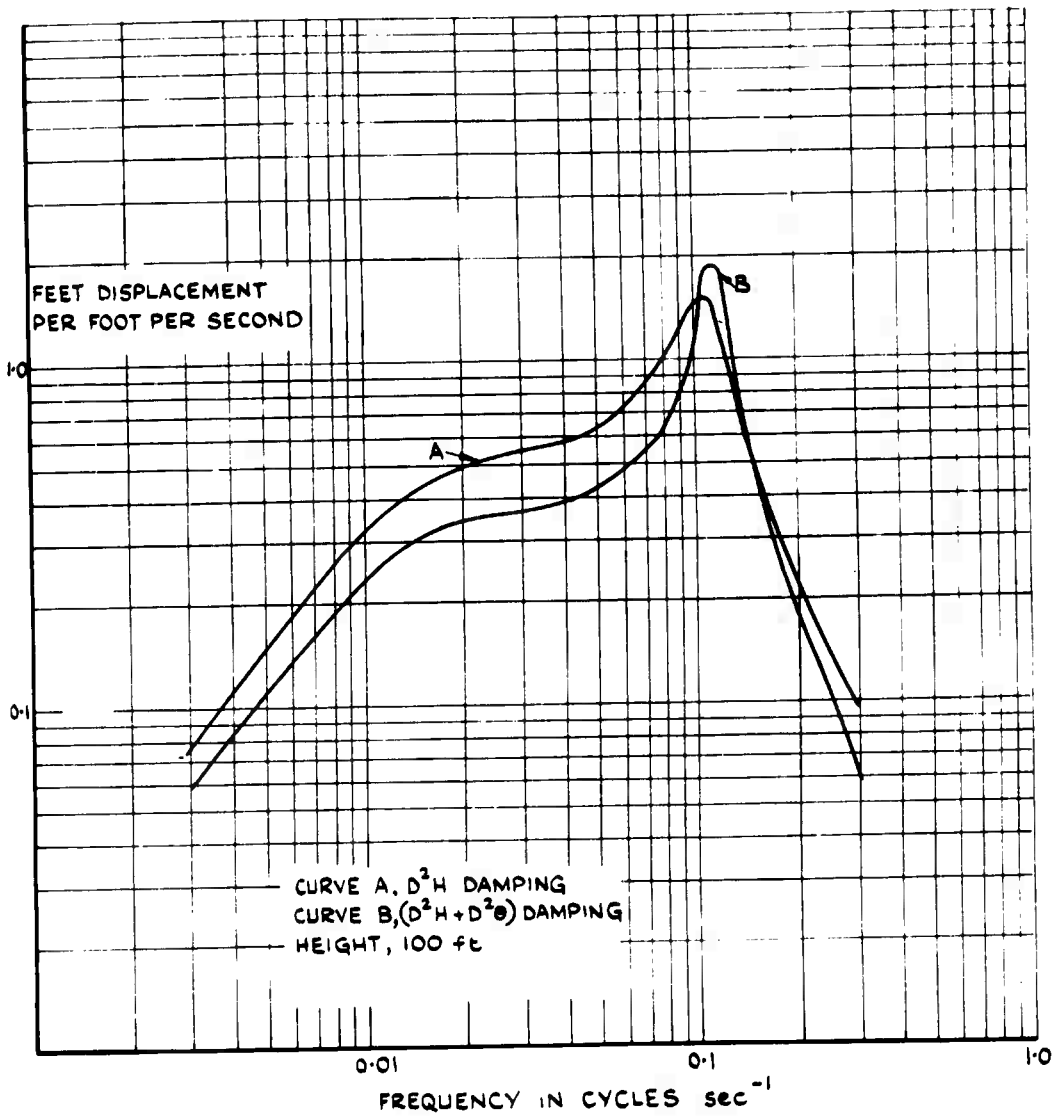


FIG. 17 FREQUENCY RESPONSE TO HORIZONTAL
WIND VARIATIONS

Fig.18

601-900038

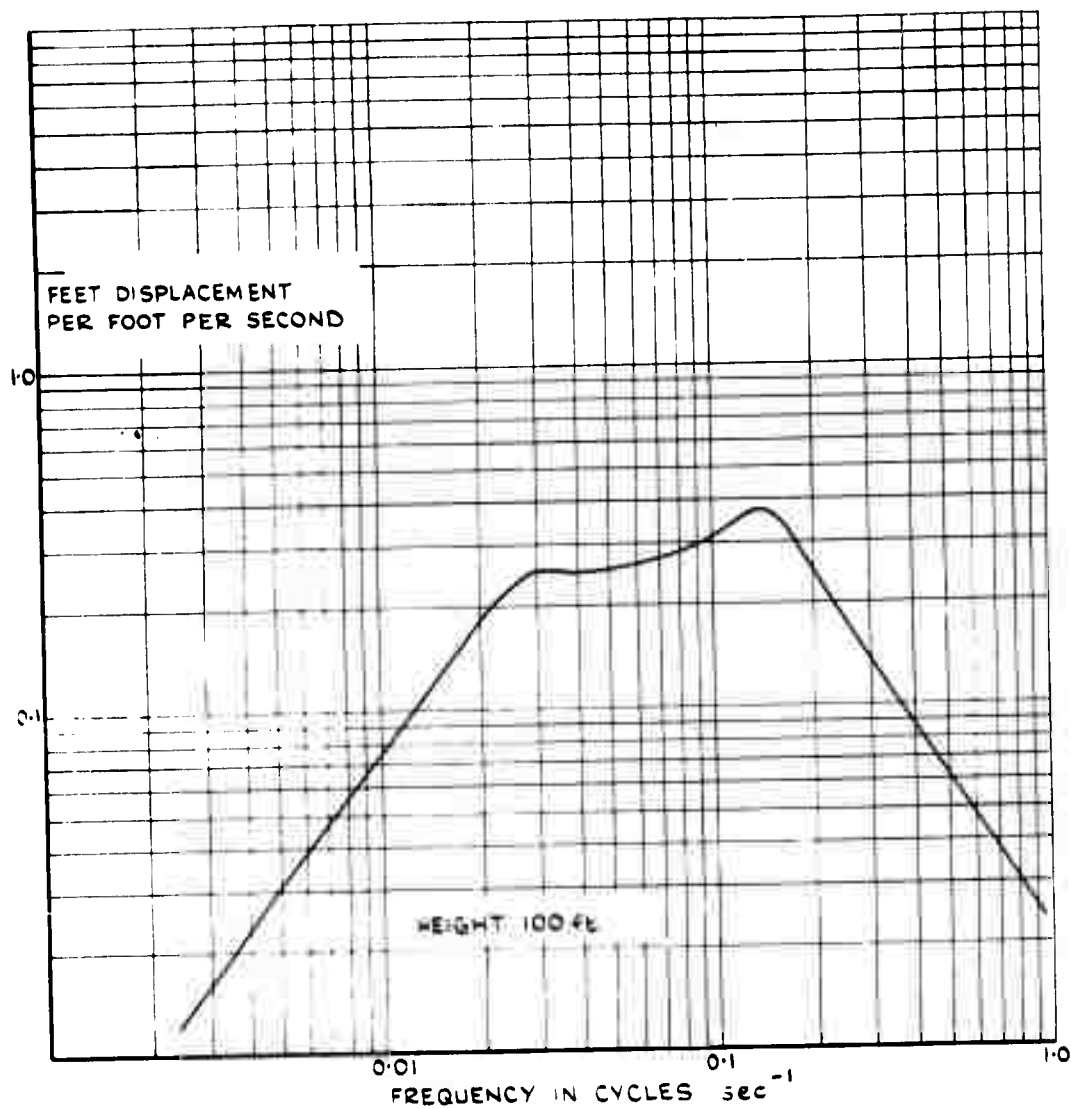


FIG.18 FREQUENCY RESPONSE TO HORIZONTAL
WIND VARIATIONS

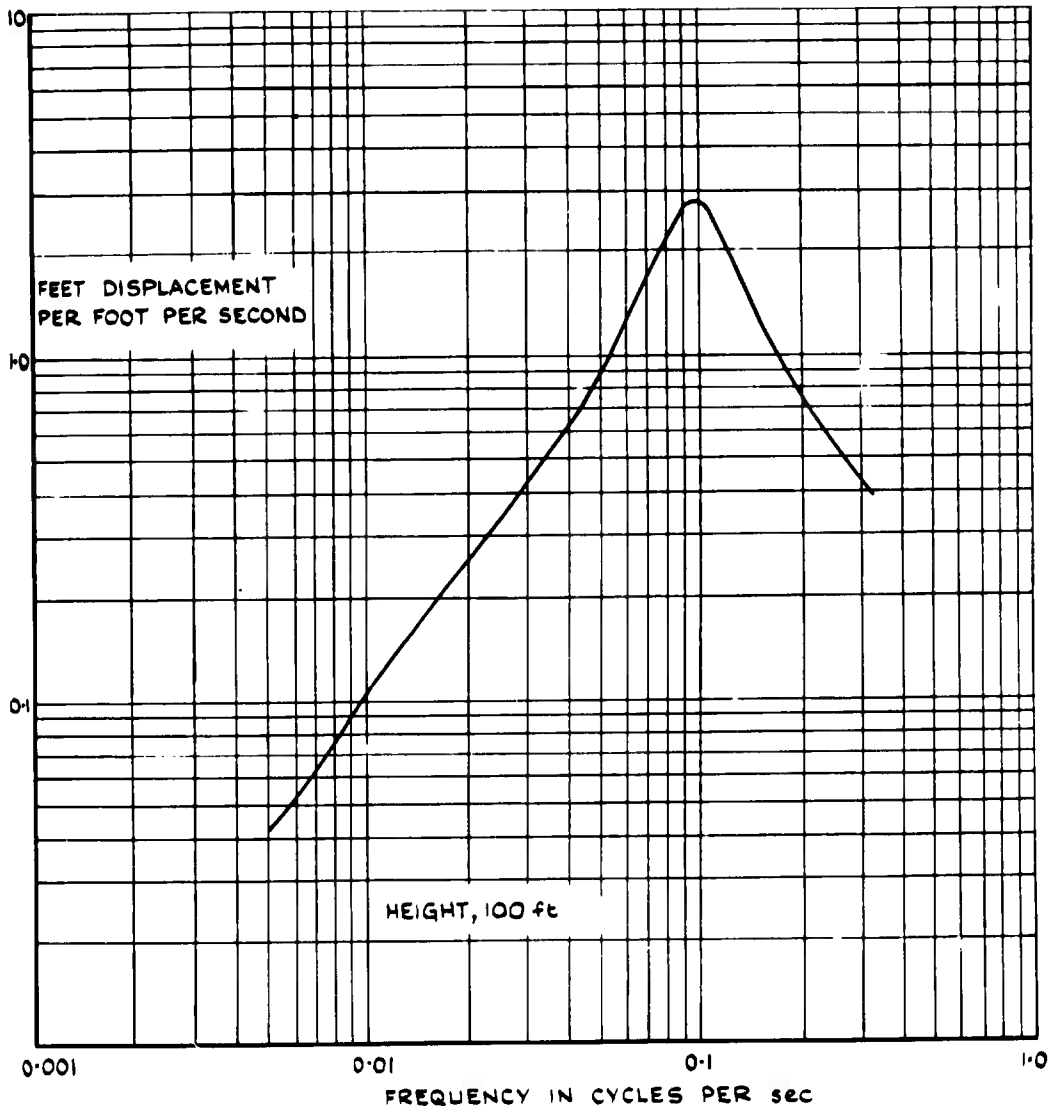


FIG.19 FREQUENCY RESPONSE TO VERTICAL WIND OF THE BASIC CONTROL SYSTEM

Fig.20

601-900040

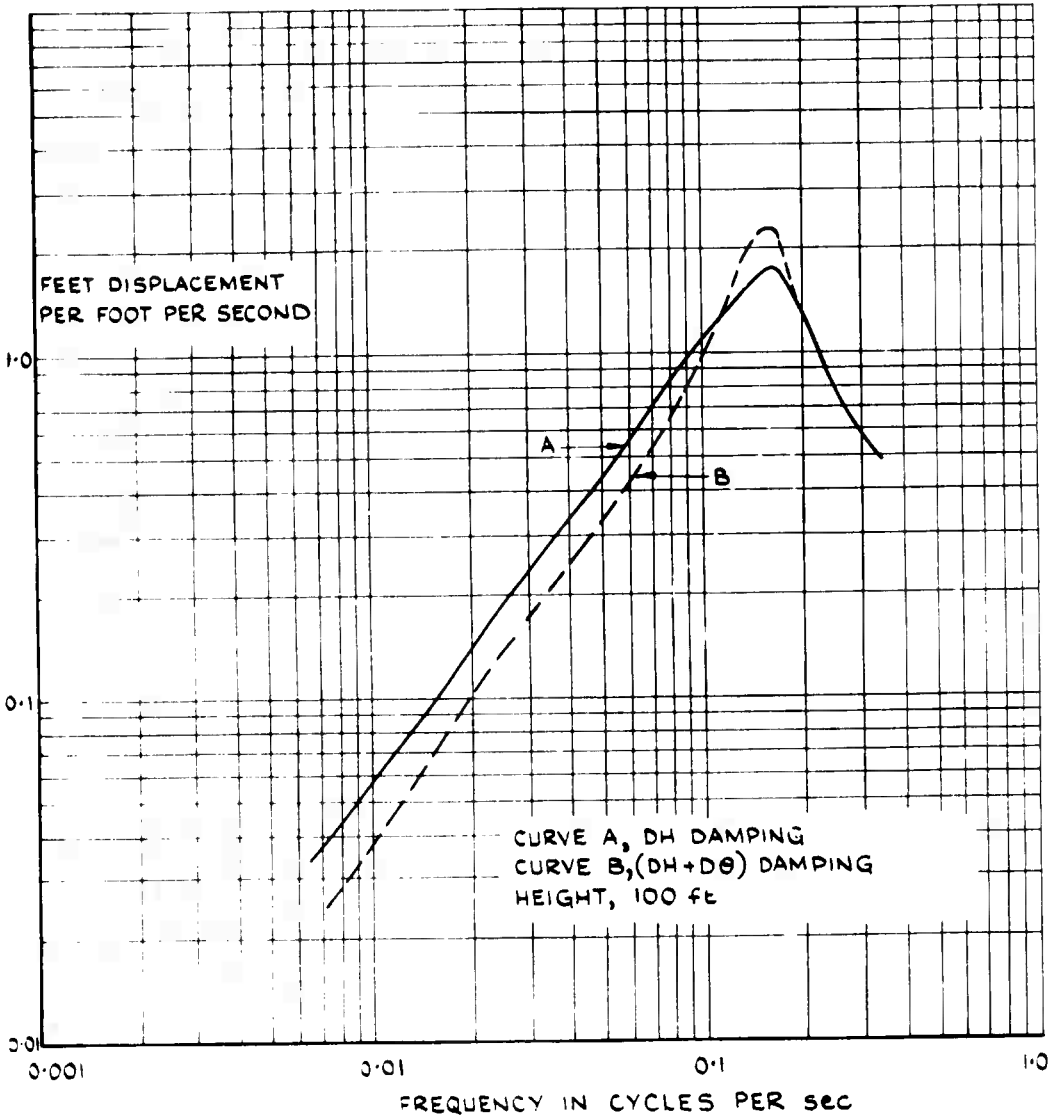


FIG. 20 FREQUENCY RESPONSE TO VERTICAL
WIND VARIATIONS

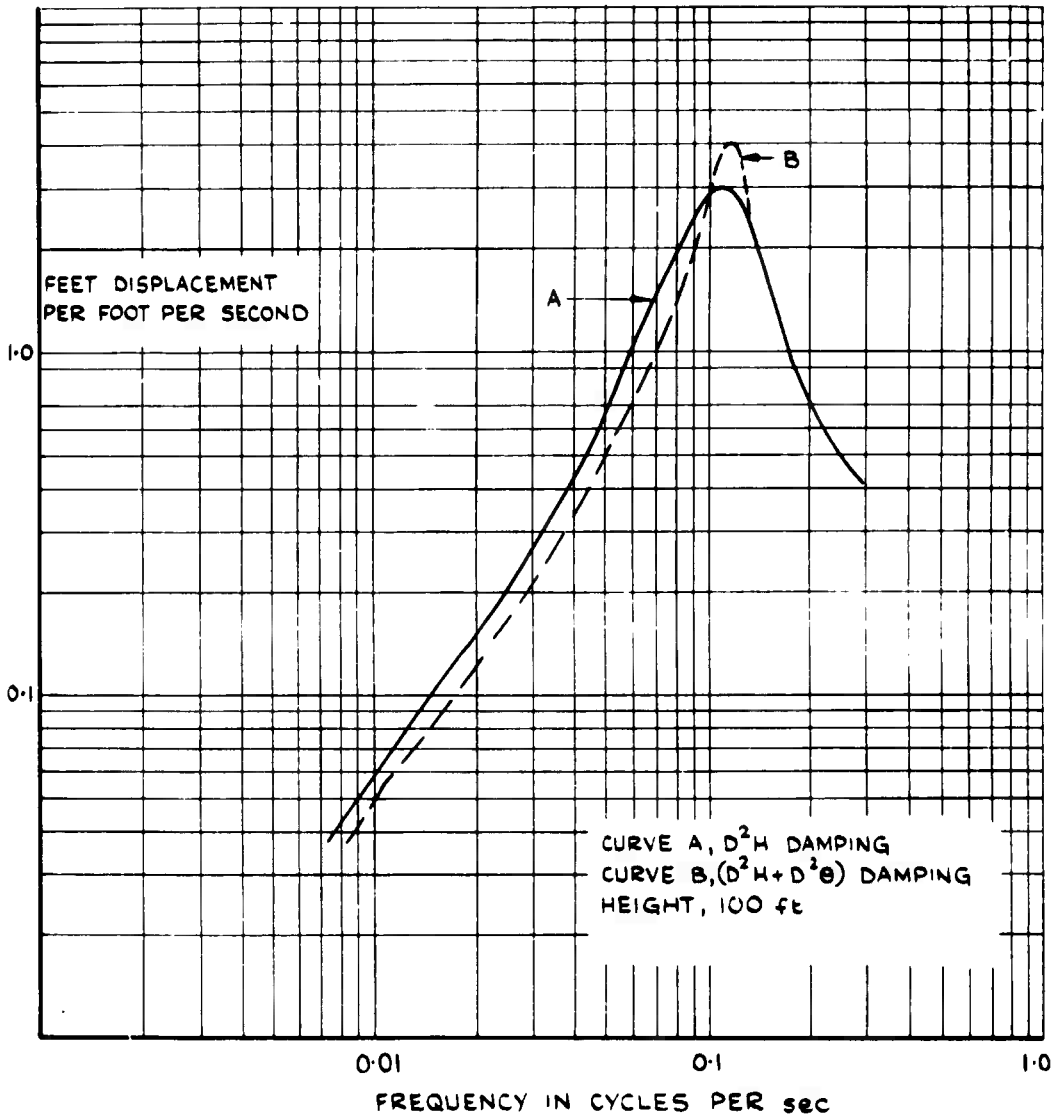


FIG. 21 FREQUENCY RESPONSE TO VERTICAL
WIND VARIATIONS

Fig.22

601-900042

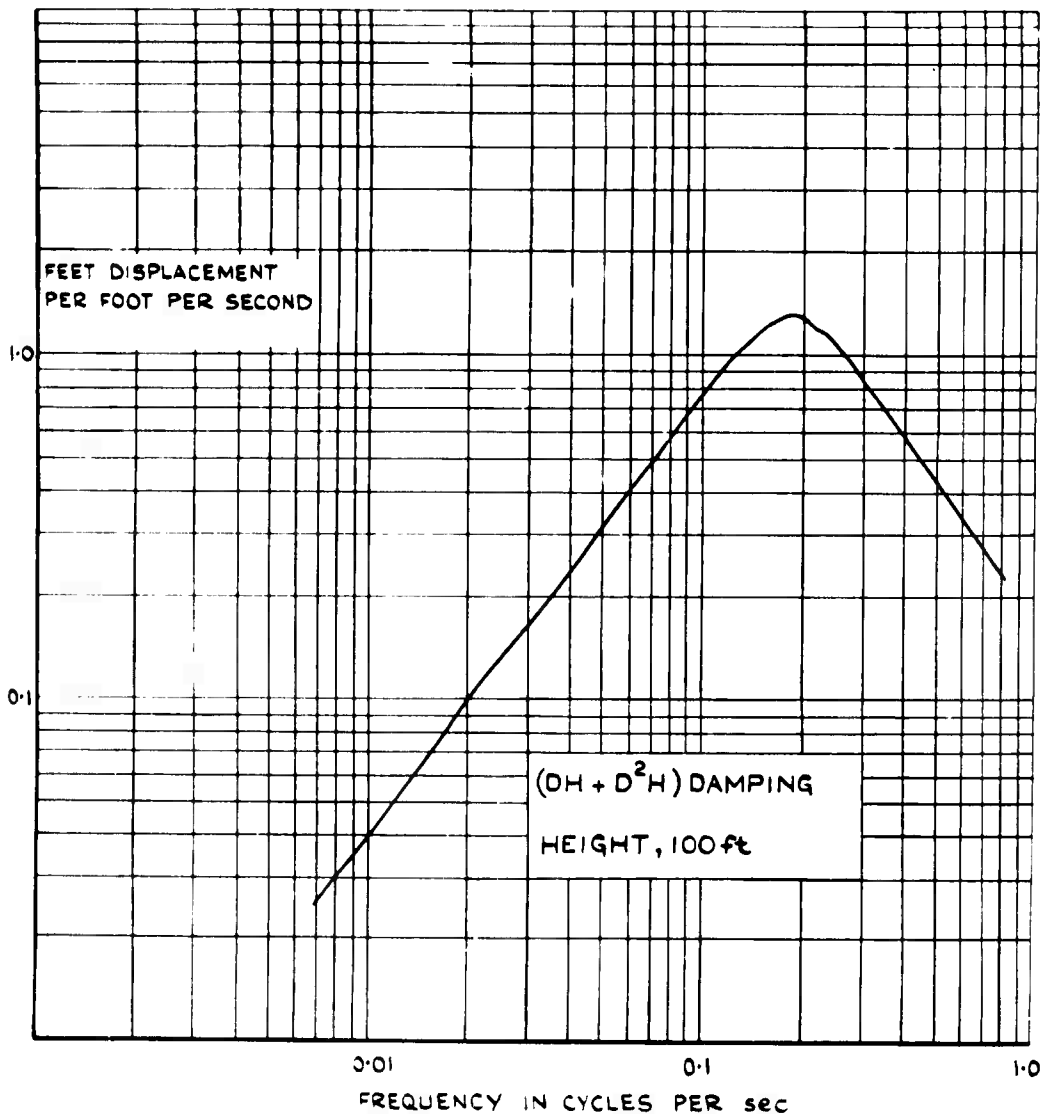


FIG. 22 FREQUENCY RESPONSE TO VERTICAL
WIND VARIATIONS

Fig.23

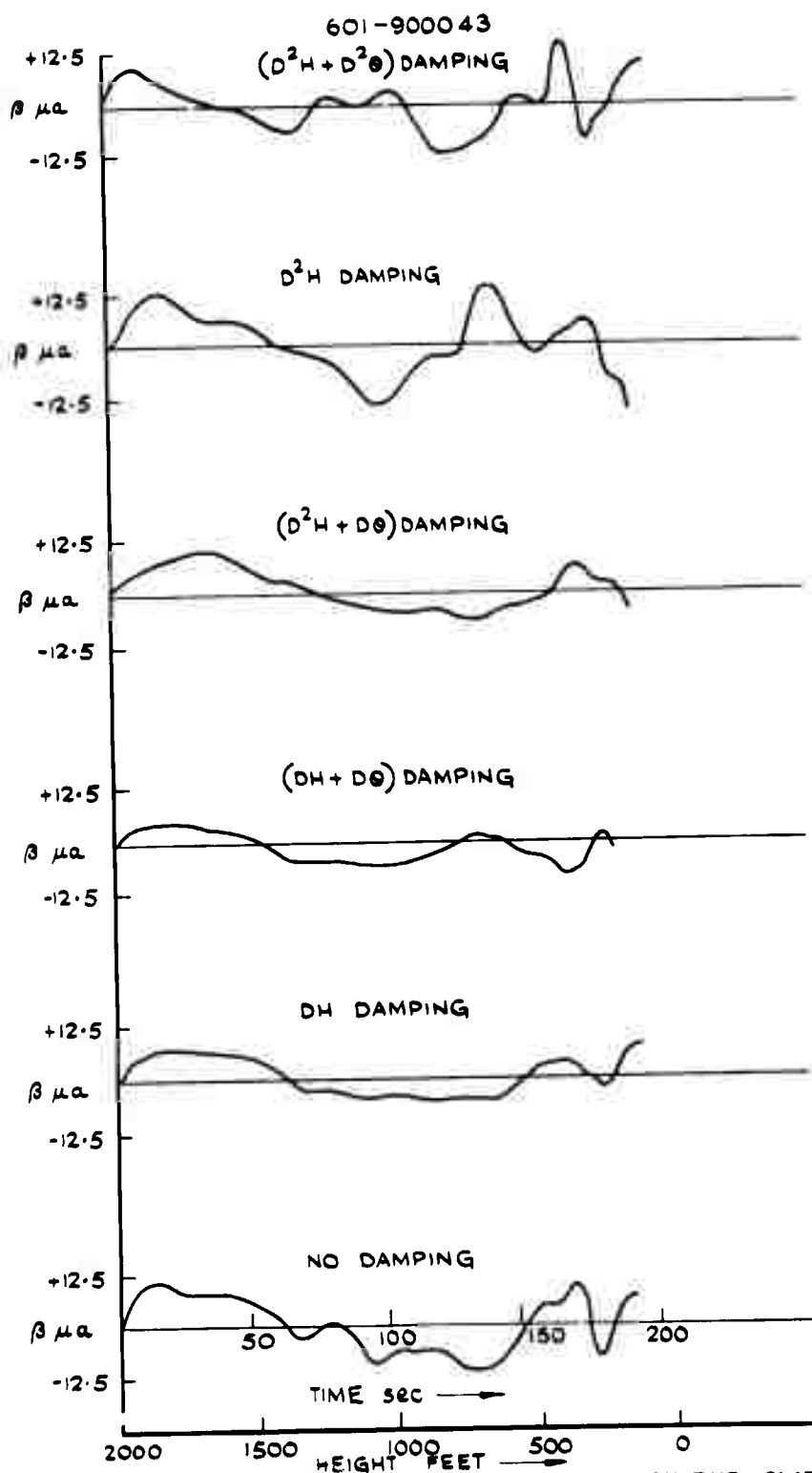


FIG.23 EFFECT OF ADDITIONAL DAMPING TERMS ON THE GLIDEPATH PERFORMANCE IN THE PRESENCE OF RANDOM HORIZONTAL WIND

Fig.24

601-900044

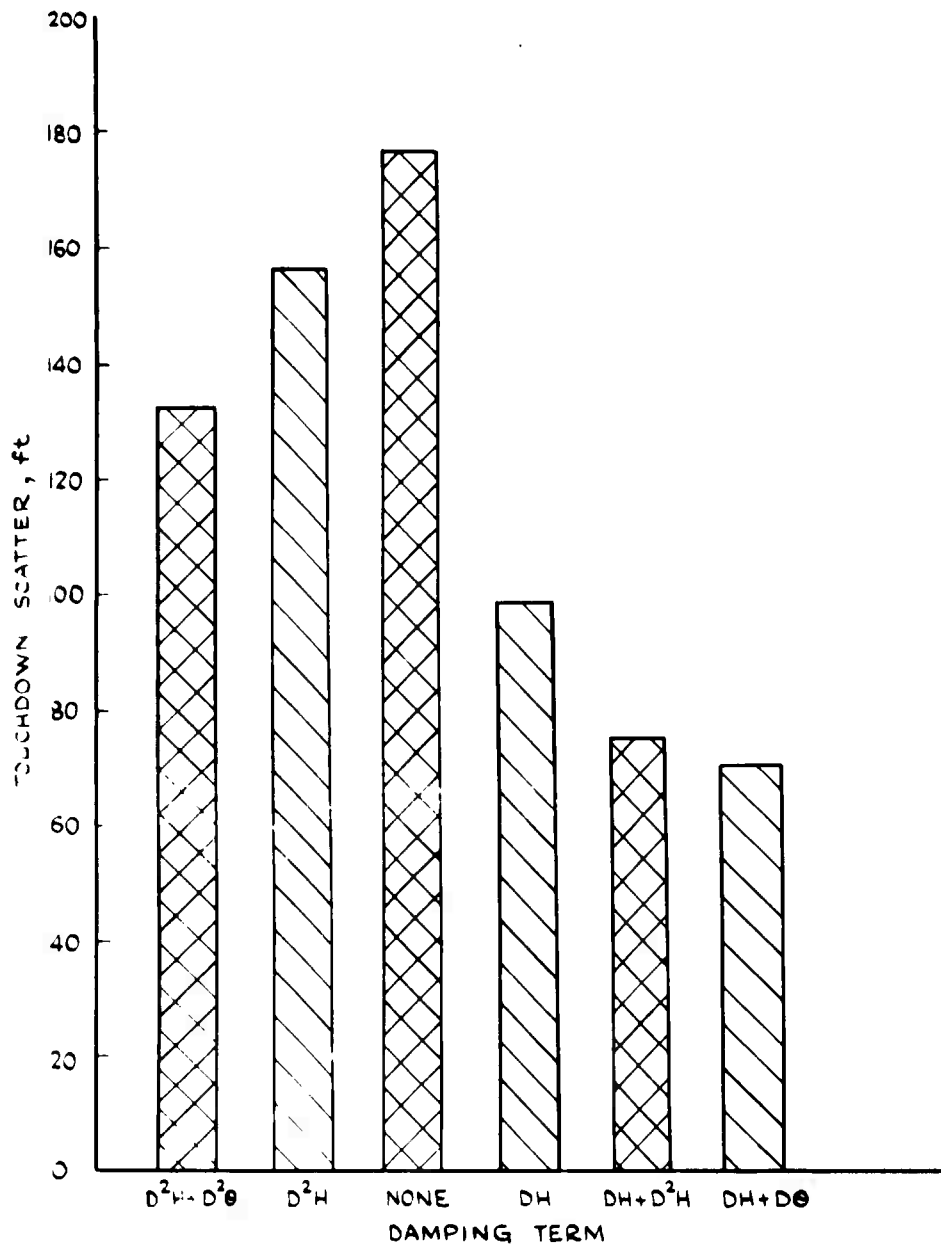


FIG.24 EFFECT OF CONTROL LAW MODIFICATIONS ON
STANDARD DEVIATION OF TOUCHDOWN RANGE

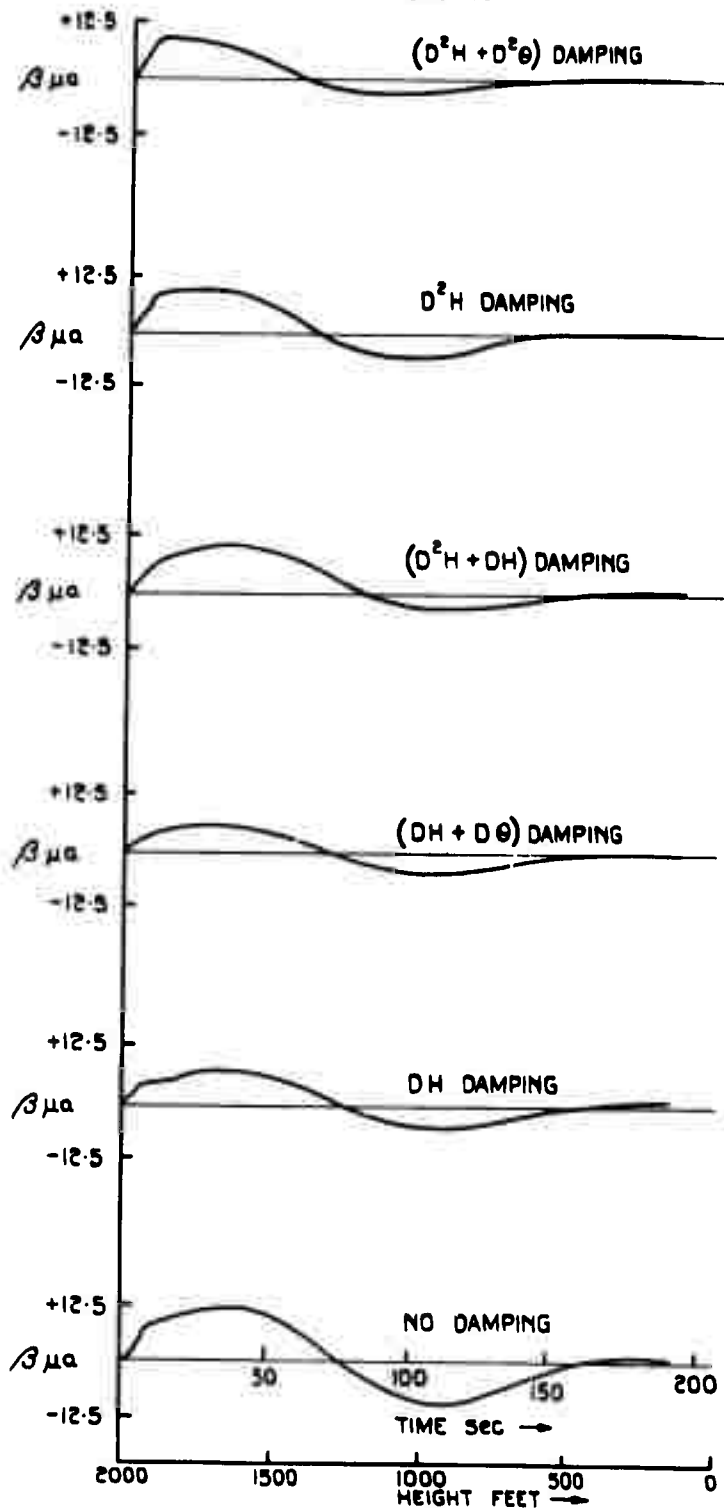


FIG. 25 EFFECT OF ADDITIONAL DAMPING TERMS ON THE GLIDEPATH PERFORMANCE IN ZERO WIND.

Fig.26

601-900046

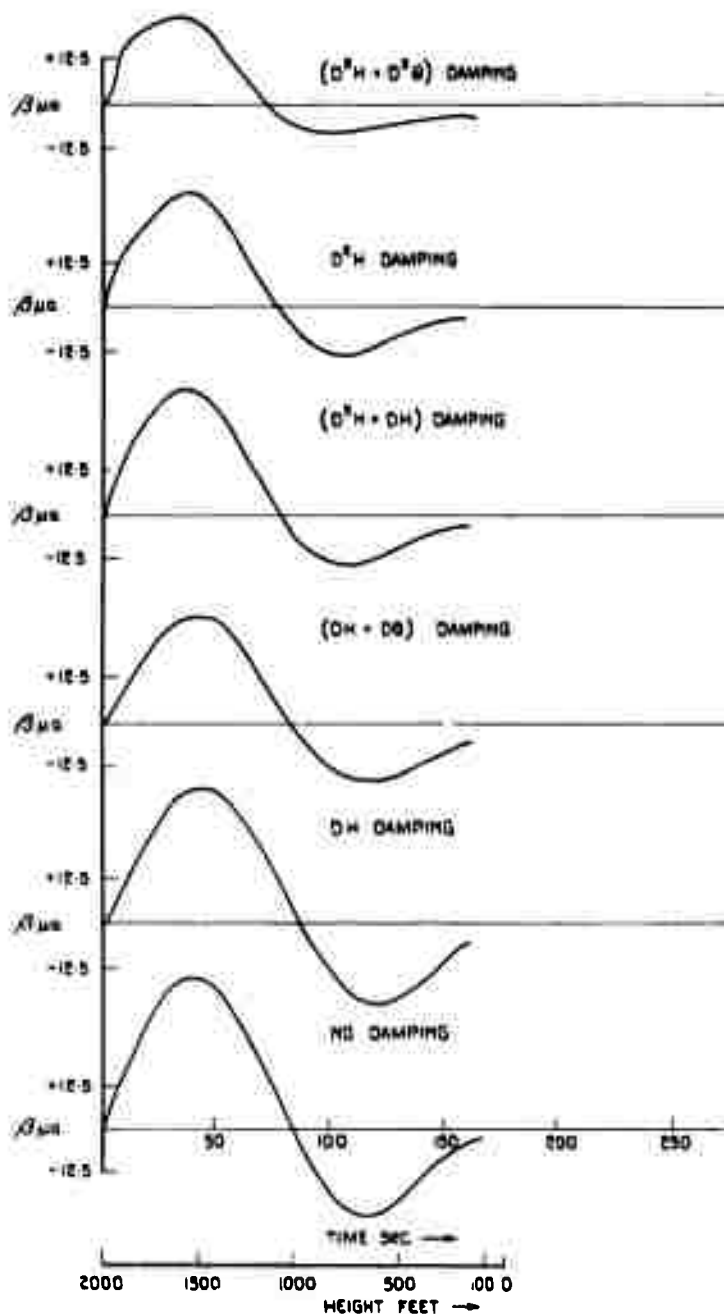


FIG.26 EFFECT OF ADDITIONAL DAMPING TERMS ON THE GLIDEPATH PERFORMANCE IN THE PRESENCE OF TAIL WIND SHEAR

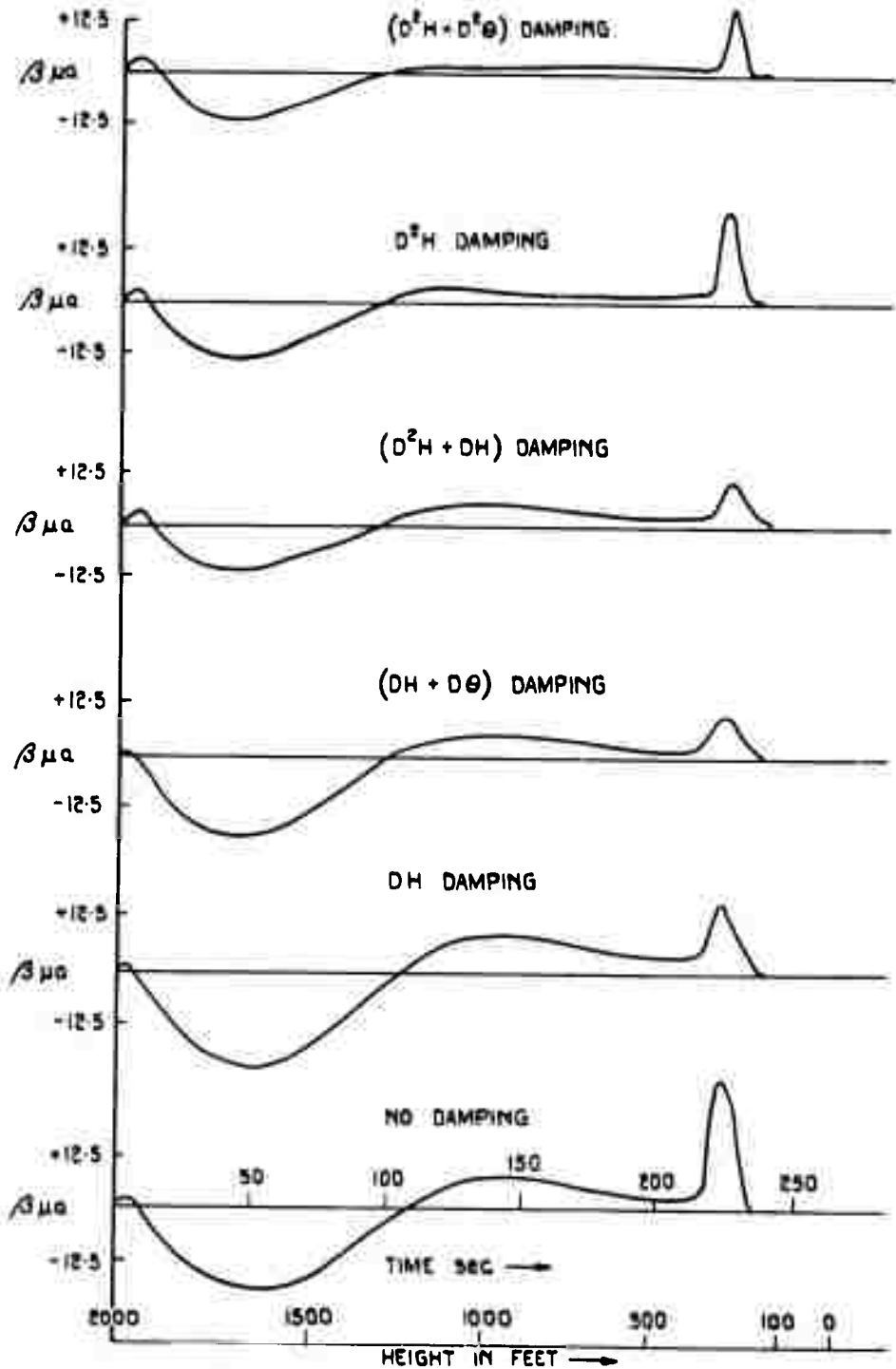


FIG.27. EFFECT OF ADDITIONAL DAMPING TERMS ON THE GLIDEPATH PERFORMANCE IN THE PRESENCE OF HEAD WIND SHEAR AND A GUST OF 5 FT/SEC AT 300 FT.

Fig.28

601-900048

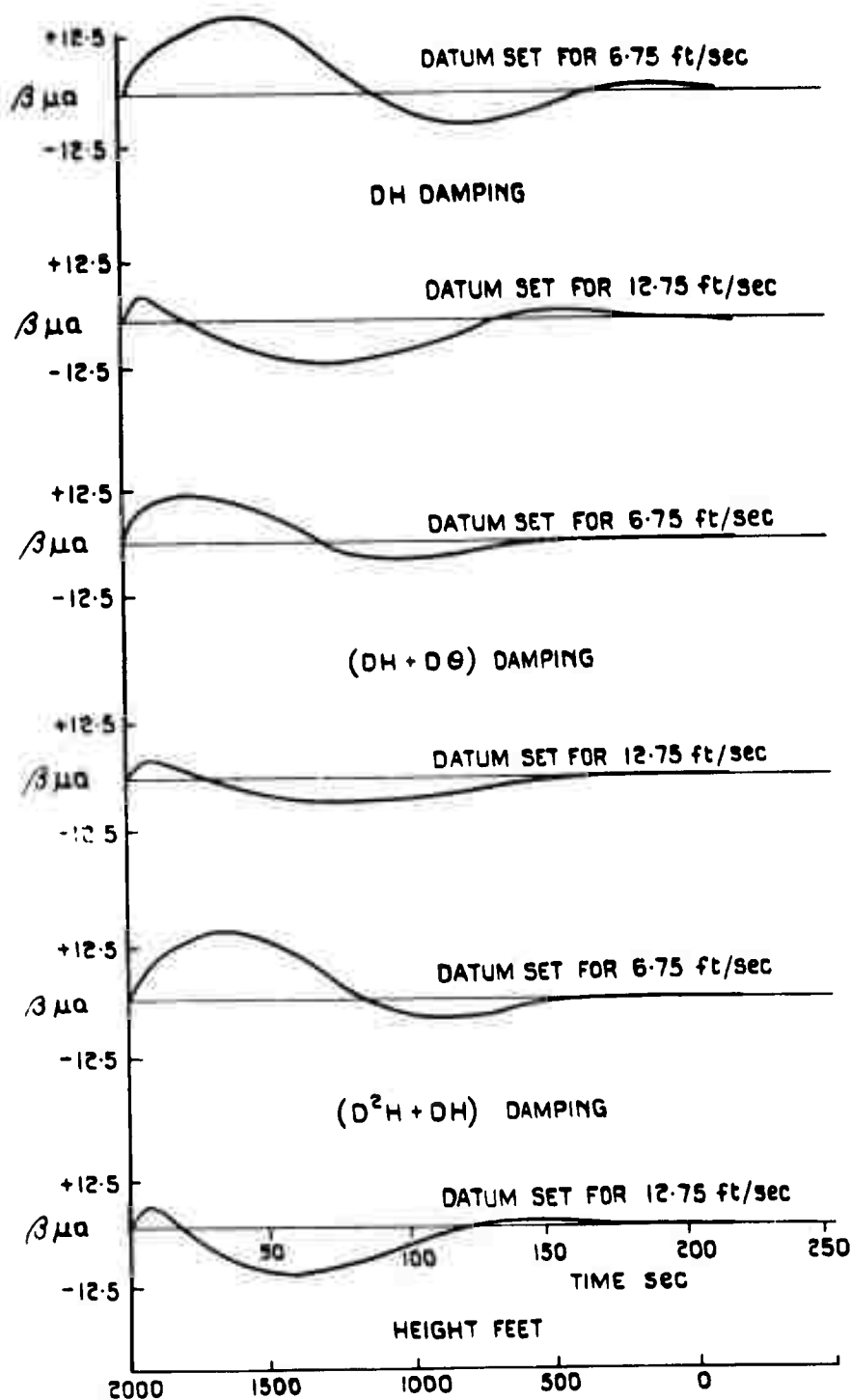


FIG.28 EFFECT OF ERROR ON RATE OF DESCENT DATUM FOR A 30° GLIDEPLATH WITH NO EXTERNAL DISTURBANCE.

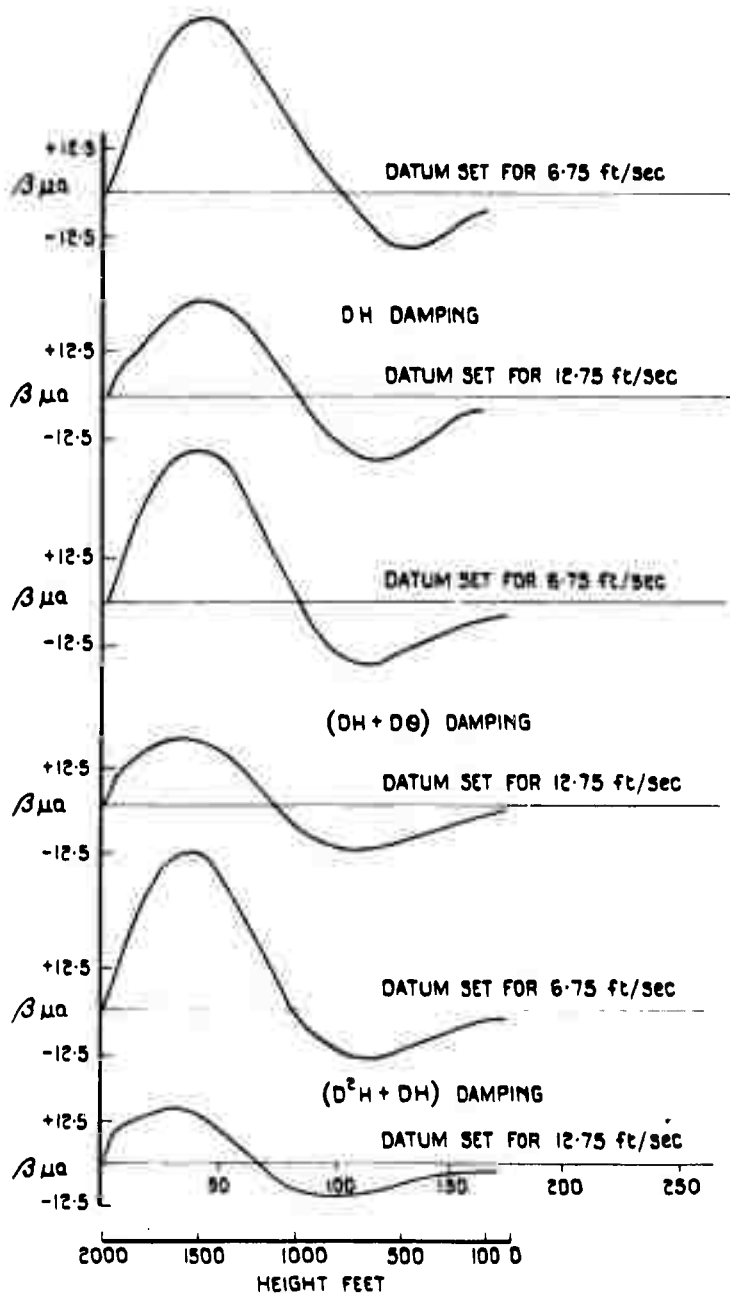


FIG.29 EFFECT OF ERROR ON RATE OF DESCENT DATUM FOR A 3° GLIDEPATH IN THE PRESENCE OF TAILWIND SHEAR

Fig.30

601 - 900050

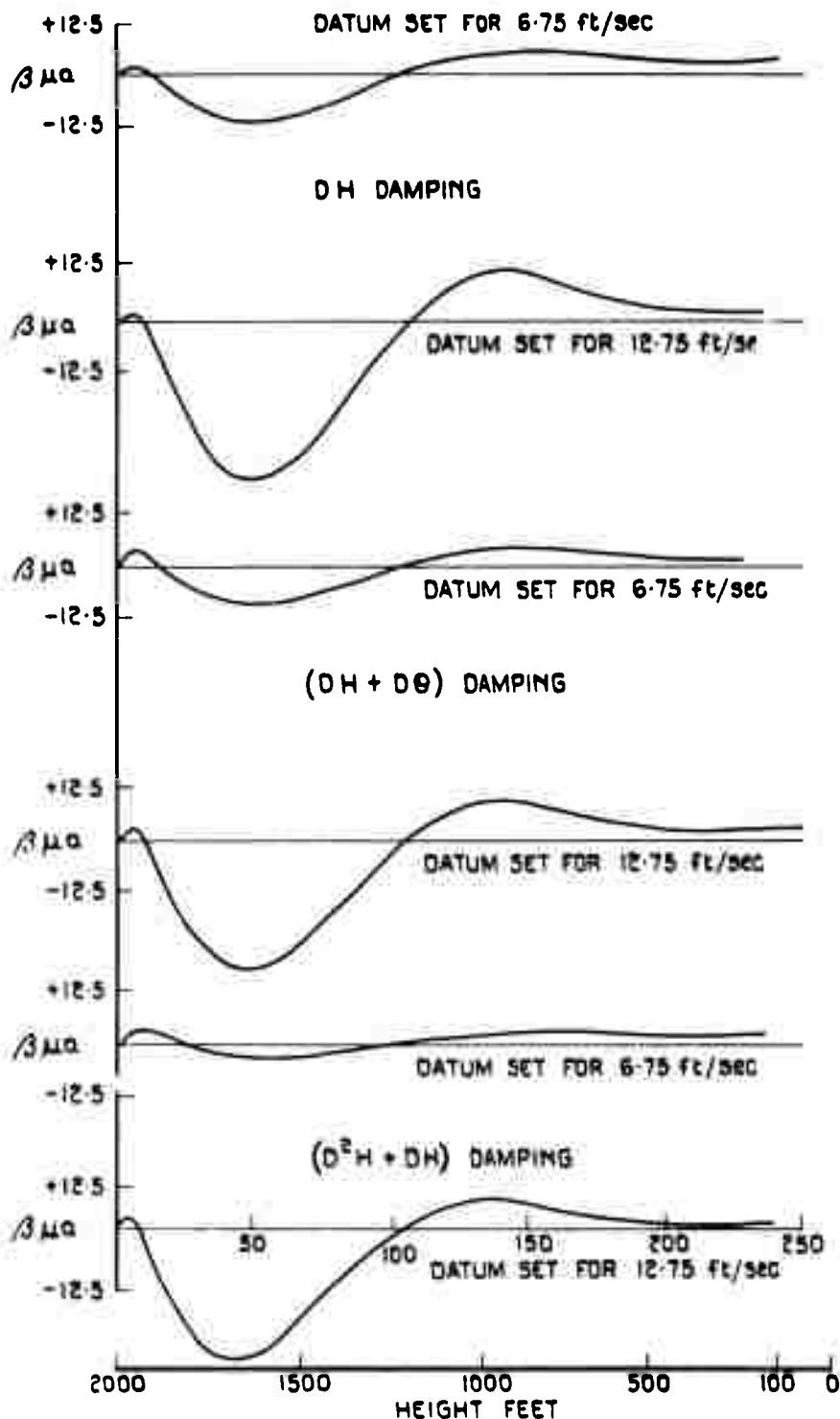


FIG. 30 EFFECT OF ERROR ON RATE OF DESCENT DATUM FOR A 3° GLIDEPATH IN THE PRESENCE OF HEADWIND SHEAR